Journal Pre-proofs

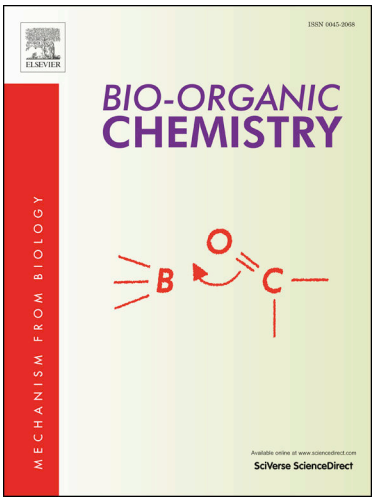

NMR for screening and a biochemical assay: identification of new FPPS inhibitors exerting anticancer activity

Manuela Grimaldi, Rosario Randino, Elena Ciaglia, Mario Scrima, Michela Buonocore, Ilaria Stillitano, Verdiana Covelli, Alessandra Tosco, Patrizia Gazzerro, Maurizio Bifulco, Manuela Rodriquez, Anna Maria D'Ursi

PII: S0045-2068(19)31112-5
DOI: https://doi.org/10.1016/j.bioorg.2019.103449
Reference: YBIOO 103449

To appear in: *Bioorganic Chemistry*

Received Date: 16 July 2019
Revised Date: 1 October 2019
Accepted Date: 14 November 2019

Please cite this article as: M. Grimaldi, R. Randino, E. Ciaglia, M. Scrima, M. Buonocore, I. Stillitano, V. Covelli, A. Tosco, P. Gazzerro, M. Bifulco, M. Rodriquez, A. Maria D'Ursi, NMR for screening and a biochemical assay: identification of new FPPS inhibitors exerting anticancer activity, *Bioorganic Chemistry* (2019), doi: https://doi.org/10.1016/j.bioorg.2019.103449

NMR for screening and a biochemical assay: identification of new FPPS inhibitors exerting anticancer activity

Manuela Grimaldi,[a,d] Rosario Randino,[a] Elena Ciaglia,[c] Mario Scrima,[a] Michela Buonocore,[a] Ilaria Stillitano,[a] Verdiana Covelli,[a] Alessandra Tosco,[a] Patrizia Gazzerro,[a] Maurizio Bifulco,[b,c] Manuela Rodriquez,[a] and Anna Maria D'Ursi[a]*

[a]*Department of Pharmacy, University of Salerno, Via Giovanni Paolo II 132, 84084, Fisciano (Salerno), Italy.*

[b]*Department of Molecular Medicine and Medical Biotechnology, University of Naples "Federico II", Via Pansini, 80131, Naples, Italy.*

[c]*Department of Medicine, Surgery and Dentistry "Scuola Medica Salernitana", University of Salerno, Via Salvatore Allende, 84081, Baronissi (Salerno), Italy.*

[d]*Institute of Polymers, Composites and Biomaterials, National Research Council of Italy, V.le J.F. Kennedy 54 - Pad. 20 Mostra d'Oltremare, 80125 Naples, Italy.*

To whom correspondence may be addressed: dursi@unisa.it

* Correspondence to:

Anna Maria D'Ursi, *Department of Pharmacy, University of Salerno, Via Giovanni Paolo II 132, 84084, Fisciano (Salerno), Italy.*

e-mail: dursi@unisa.it, Phone:+39089969748

Abstract

Farnesyl pyrophosphate synthase (FPPS) is a crucial enzyme for the synthesis of isoprenoids and the key target of nitrogen-containing bisphosphonates (N-BPs). N-BPs are potent and selective FPPS inhibitors that are used in the treatment of bone-related diseases, but have poor pharmacokinetic properties.

Given the key role played by FPPS in many cancer-related pathways and the pharmacokinetic limits of N-BP, hundreds of molecules have been screened to identify new FPPS inhibitors characterized by improved drug-like properties that are useful for broader therapeutic applications in solid, non-skeletal tumours.

We have previously shown that N6-isopentenyladenosine (**i6A**) and its related compound N6-benzyladenosine (**2**) exert anti-glioma activity by interfering with the mevalonate pathway and inhibiting FPPS. Here, we report the design and synthesis of a panel of N6-benzyladenosine derivatives (compounds **2a-m**) incorporating different chemical moieties on the benzyl ring. Compounds **2a-m** show in vitro antiproliferative activity in U87MG glioma cells and, analogous to the bisphosphonate FPPS inhibitors, exhibit immunogenic properties in *ex vivo* γδ T cells from stimulated peripheral blood mononuclear cells (PBMCs). Using saturation transfer difference (STD) and quantitative ^{1}H nuclear magnetic resonance (NMR) experiments, we found that **2f,** the N6-benzyladenosine analogue that includes a tertbutyl moiety in the *para* position of the benzyl ring, is endowed with increased FPPS binding and inhibition compared to the parent compounds **i6A** and **2**.

N6-benzyladenosine derivatives, characterized by structural features that are significantly different from those of N-BPs, have been confirmed to be promising chemical scaffolds for the development of N-BP FPPS inhibitors, exerting combined cytotoxic and immunostimulatory activities.

Graphical abstract

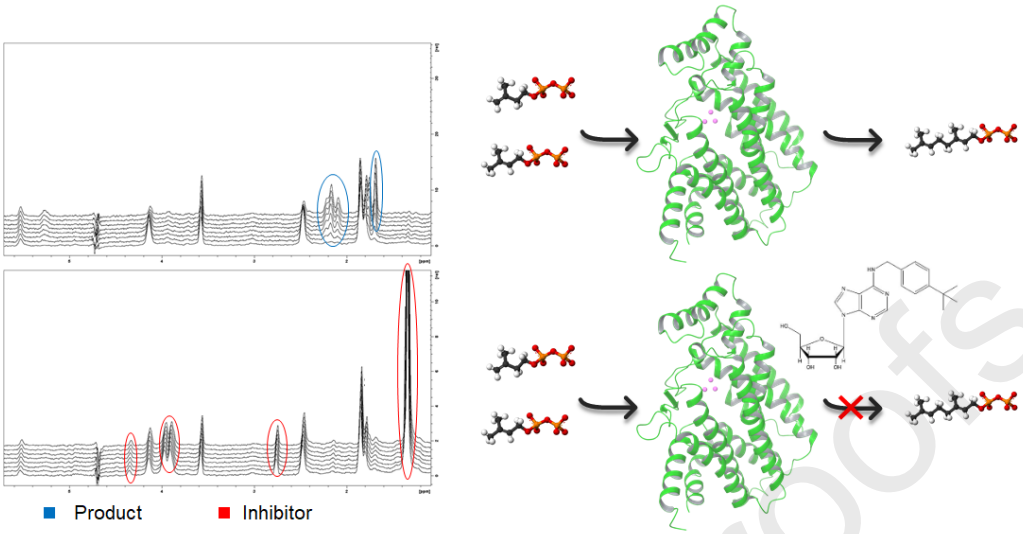

Keywords

FPPS, isoprenoids, adenosine derivatives, NMR enzymatic assay

1. Introduction

Farnesyl pyrophosphate synthase (FPPS) is a key enzyme involved in the mevalonate (MVA) pathway and prenylation of downstream proteins; it catalyses the two-step synthesis of the C15 isoprenoid farnesyl pyrophosphate (FPP), a crucial precursor for the synthesis of several classes of essential metabolites, such as sterols, ubiquinones, and carotenoids.[1-3]

FPPS has been implicated in many cancer-related pathways[4, 5] and plays a significant role in the maintenance of the neoplastic malignant phenotype. In particular, we recently documented the deregulated expression and activity of FPPS in a cohort of stage III-IV glioma patients; in primary glioblastoma-derived cells, we found FPPS alterations, exhibiting a linear correlation with canonical oncogenic signalling pathways such as signal transducer and activator of transcription 3 (STAT3), extracellular signal-regulated kinase (ERK), and protein kinase AKT.[6]

Nitrogen-containing bisphosphonates (N-BPs) are potent and selective inhibitors of FPPS that are used for the treatment of bone-related tumours and osteoporosis diseases.[7-10] Due to their ability to induce stimulation of innate δ T cytotoxic antitumoural cells, N-BPs are also used in immunotherapy-based cancer treatment.[11-14] Despite their potency, N-BPs suffer from poor pharmacokinetics, exhibiting almost negligible distribution to non-skeletal tissues and rapid clearance from systemic circulation.[7]

Given the important role played by FPPS in cancer manifestation and progression,[15] hundreds of molecules have been tested in search of new FPPS inhibitors with improved drug-like properties that are useful for broader therapeutic applications in solid, non-skeletal tumours.[16, 17] In particular, powerful uncharged FPPS inhibitors targeting an allosteric pocket of FPPS were recently identified using fragment-based screening by nuclear magnetic resonance (NMR) and X-ray crystallographic methods.[18, 19]

In our previous investigation, including an *in silico* inverse virtual screening, NMR experiments and in vitro enzymatic assays, FPPS was found to be a valuable target for the structural binding of N6-isopentenyladenosine (**i6A**) (**1** in Figure 1).[20] Compound **i6A** is a modified nucleoside belonging to the cytokine family. It is involved in the control of many processes in plants[21-24] and exerts in vitro and in vivo antitumoural and immunomodulatory activities.[25-31] Interestingly, in many experiments, the cytotoxicity and anti-proliferative activity of **i6A** was shown to be associated with alterations in FPPS expression and activity.[31-33]

Encouraged by the preliminary data on FPPS-**i6A** binding, we decided to synthesize and test **i6A** analogues, including those with different substituents at the N6position of adenosine. The N6-benzyladenosine derivative (**2**, Figure 1),[30] where a benzyl moiety on the adenosine ring replaced the isopentenyl, confirmed the ability of **2** to bind and inhibit FPPS and exhibited greater cytostatic and anti-proliferative activities than those of the parent compound **i6A**.

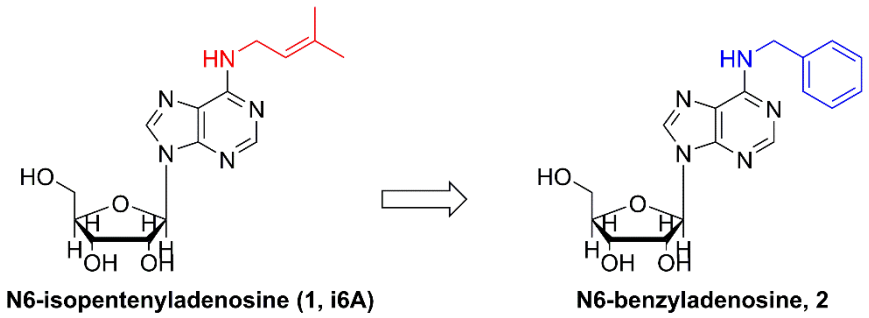

Figure 1. Chemical structures of **i6A** (**1**) and N6-benzyladenosine (**2**).

Intending to obtain N6-benzyladenosine derivatives endowed with improved FPPS binding, in this report, we describe the efforts to design, synthesize and screen a panel of compounds resulting from the introduction of different chemical moieties in the *para* position of the N6-benzyl ring of **2** (**2a-m**, Figure 2).

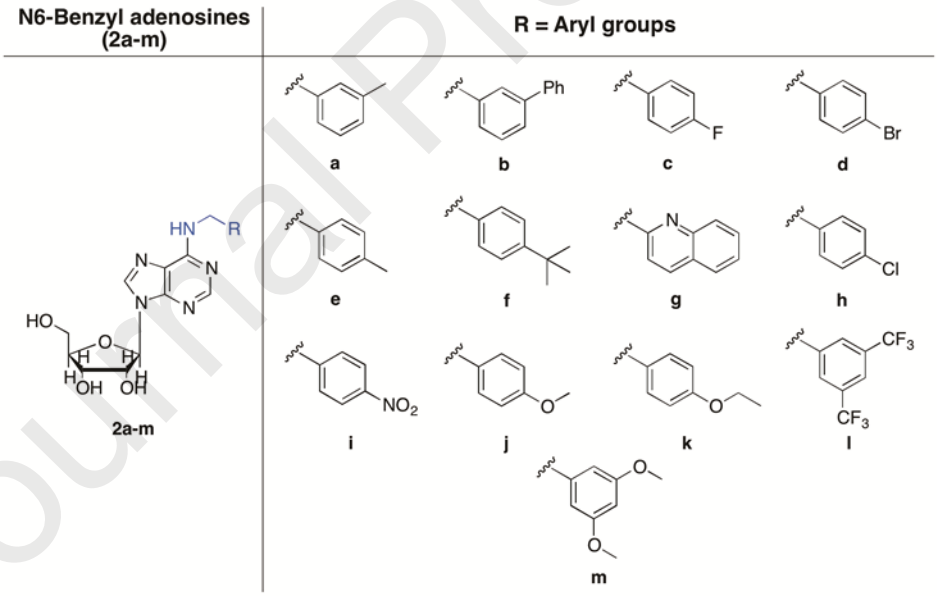

Figure 2. Chemical structures of N6-benzyladenosine derivatives (**2a-m**).

We employed saturation transfer difference (STD) NMR experiments to study compounds **2a-m** interacting with the FPPS binding pocket; moreover, we developed an innovative NMR-based FPPS enzymatic assay based on quantitative ^{1}H-NMR measurements of FPPS substrates

vs. products. Finally, we confirmed the effects of compounds **2a-m** on FPPS by measuring their immunostimulatory effects on peripheral T-lymphocytes, analogous to bisphosphonate FPPS inhibitors.[14]

2. Results

2.1 Design of N6-benzyladenosine analogues (2a-m)

The description of the active site of the FPPS enzyme, according to the numerous crystal structures deposited in the Brookhaven PDB (https://www.rcsb.org/; https://www.uniprot.org/uniprot/P14324), is consistent with the existence of i) an allylic sub-pocket where the pyrophosphate moiety of DMAPP/GPP interacts with the enzyme via Mg^{2+}-mediated interactions and ii) an IPP sub-pocket where the pyrophosphate moiety of IPP interacts with basic residues through direct salt bridge (K57, R60, R113) or water-mediated (R112, R351) interactions.[17, 34, 35] We have previously demonstrated that **i6A** and its derivative N6-benzyladenosine (**2**, Figure 1) bind to the FPPS catalytic site, inducing moderate inhibition of its enzymatic activity.[20, 30] Based on our molecular docking calculations, in the most represented binding poses, the isopentenyl moiety of **i6A** and the benzyl ring of **2** interact with the allylic sub-pocket in a region that is large enough to contain additional bulky substituents. To obtain more active FPPS ligands, we designed a panel of compounds carrying substituents with different steric hindrances on the N6-adenosine benzyl ring. The designed compounds were docked in the FPPS binding site using AutoDock Vina (version 1.1.2).[36] An FPPS X-ray structure that included three Mg^{2+} ions essential for enzymatic activity was selected from the PDB (ID code: 5YGI) following the criteria explained in our previous works.[20, 30] The binding energies of compounds **2a-m** resulting from the molecular docking calculations are reported in the Supplementary Information (Table S1). Compounds **2f**, **2g**, and **2i,** characterized by the best docking score parameters, show improved FPPS binding compared

to the parent compounds **i6A** and **2**. Analysis of the most representative binding poses (Figure 3a-b) indicates that all the molecules have a similar orientation: the ribosyl sugar and adenine rings are located in the highly charged DMAPP sub-pocket, exploiting metal interactions with an Mg^{2+} ion, with additional stabilizing interactions involving Asp residues in the conserved aspartate-rich motif. The *para*-substituted benzyl ring occupies a large hydrophobic sub-pocket and engages in cation-π interactions with F98, F99, Y204, and L100.

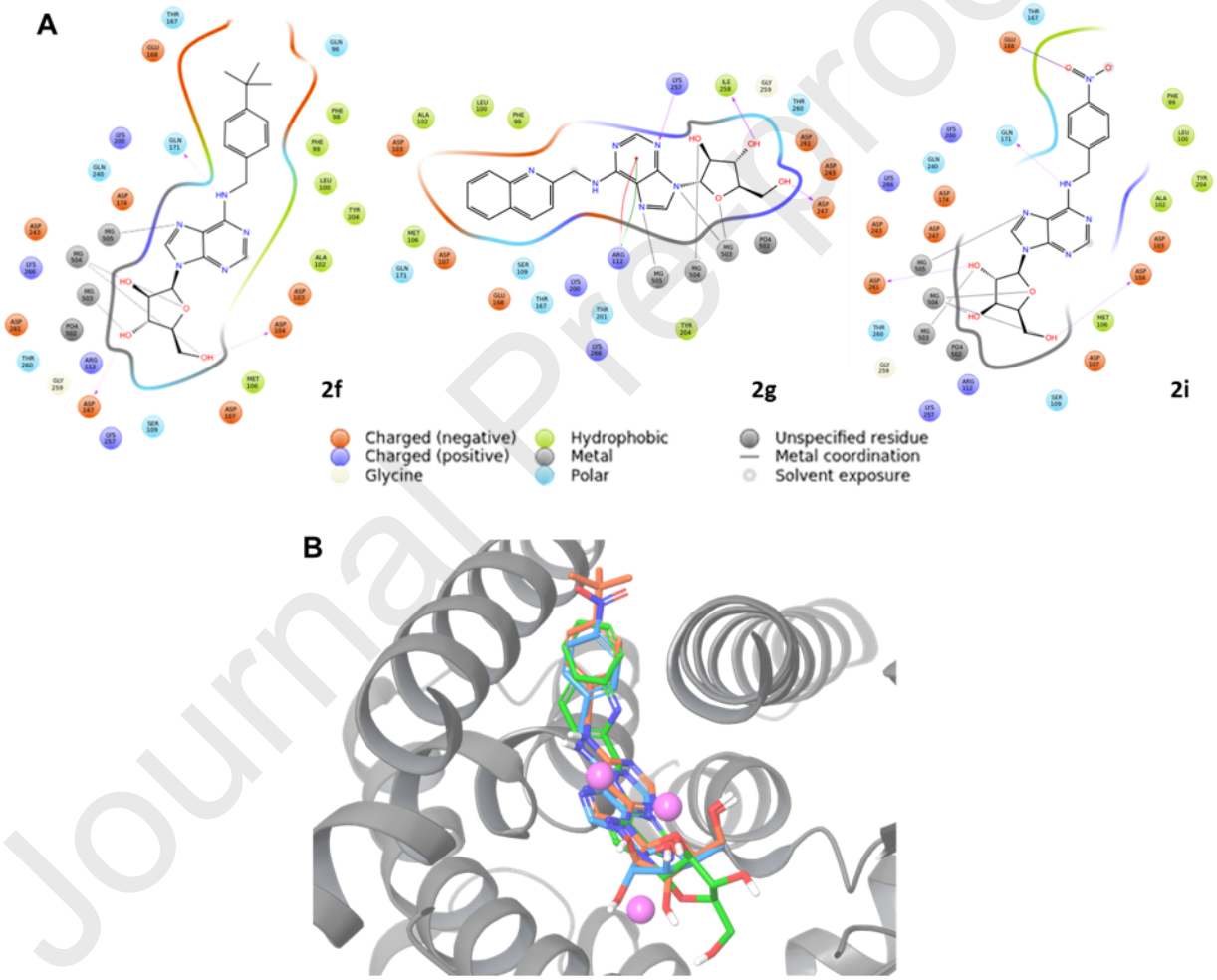

Figure 3. a) Two dimensional interaction panel showing interactions between **2f**, **2g**, and **2i** and the FPPS binding site (PDB ID 5YGI) as derived from molecular docking calculations. **b)** The 3D superposition of the best binding poses derived from the docking calculations of **2f**

(orange), **2g** (blue) and **2i** (green) with the FPPS (PDB ID: 5YGI) binding site. The FPPS backbone is shown as a grey ribbon.

2.2 Chemistry

Adenosine represents a very suitable scaffold for chemical modifications; its high polarity confers a peculiar solubility profile to its derivatives. Several methods for the preparation of ring-substituted N6-benzyladenosines have been previously described.[37-40] Generally, these synthetic procedures consist of the direct reaction of 6-chloropurine riboside (**3**) with the appropriate primary benzylamine. Conventional heating is used for several hours in an alcoholic solvent with an excessive amount of triethylamine (TEA)[24, 41-44] (Figure 4). By following this procedure, we first synthesized the N6-benzyladenosine derivatives by heating **3** with three eq. of benzylamine (BA) in ethanol for 3 h at 80°C; we obtained compound **2** in 55% yield (Table S2, entry **1**, see Supplementary Information).

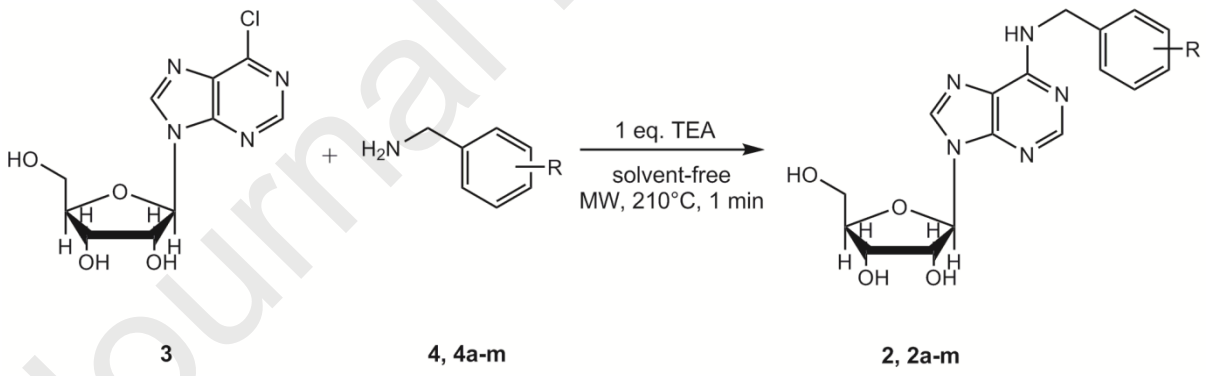

Figure 4. Synthesis of N6-benzyladenosine and derivatives **2a-m**.

Microwave-assisted (MW) synthetic protocols have been widely used as an alternative to conventional heating synthetic methods to shorten the reaction time and with respect to green chemistry and atom economy principles.[45-48]

Several MW-assisted protocols for the synthesis of N6-benzyladenosine derivatives have been previously described[46, 49]; however, by applying experimental procedures earlier developed in our laboratory[45, 50] and to optimize the reaction conditions, we decided to set up a new MW-assisted procedure by systematically modifying the reaction parameters.

First, the temperature, MW irradiation power, reaction time, and solvent were modified. A 99% conversion of 6-chloropurine riboside into **2** was obtained by heating **3** in ethanol for 5 min under MW irradiation at 180°C in the presence of three eq. of TEA, leading to **2** in 95% isolated yield (Table S2, entry **7**, see Supplementary Information). In an attempt to reduce the reaction time, we found that after irradiation for just 1 min at 210°C, the conversion of **3** into **2** was 93% (90% isolated yield, Table S2, entry **8** see Supplementary Information). Prolonged irradiation time at 210°C led to a significant increase in by-products (Table S3, entries **9-12** see Supplementary Information).

These encouraging results led us to investigate the potential effect exerted by the solvent (testing both green solvents and solvent-free conditions) modulating the reactant as well as the TEA stoichiometry. The effect of solvent and BA equivalents for the synthesis of **2** are reported in Table S2 in the Supplementary Information. Reducing the BA equivalents to 1 eq. in the presence of just one eq. of TEA and switching from EtOH to an ionic liquid and then to H_2O led to improved yields. Nevertheless, solvent-free conditions (Table S3, entry **16** see Supplementary Information) led us to reach the best results (98% conversion and 94% isolated yield), merging the most successful conditions previously reported (Table S2 for entries **7** and **8**, see Supplementary Information), irradiating **3** for just 1 min at 300 W and 210°C. These results suggest that the equimolar ratio of BA, TEA, and **3** in solvent-free conditions represent the most suitable, versatile settings for the MW-assisted synthesis of N6-benzyladenosines with respect to green chemistry and atom economy principles.[47]

These new, faster and more efficient conditions encouraged us to extend our method to different BAs (Table 1). Additionally, in these cases, the MW irradiation dramatically reduced the conversion time, improving the yields and purity of the desired N6-substituted adenosine analogues **2a-m**.

Compound	Yield (%)[a]
2a	92
2b	89
2c	92
2d	88
2e	89
2f	91
2g	87
2h	90
2i	88
2j	88
2k	84
2l	90
2m	89

[a]Yields were evaluated on the isolated product.

Table 1. Synthesis of compounds **2a-m** by using the optimized MW-assisted methodology.

2.3 FPPS-ligand interaction: NMR analysis

Compounds **2a-m**, designed and synthesized as previously described, were characterized by measuring standard ^{1}H monodimensional, 2D HSQC (H-1/X correlation via double INEPT transfer) and 2D HMBC (H-1/X correlation via heteronuclear zero and double quantum) NMR experiments in the solvent MeOD. The ^{1}H and ^{13}C chemical shift assignments of compounds **2a-m** are reported in Figures S1-S14 (Supplementary Information). Then, compounds **2a-m** were screened for their ability to bind to the FPPS enzyme by recording STD NMR experiments.[51, 52] STD is a powerful NMR technique that is used for the identification of protein-ligand interactions and the determination of protein-ligand dissociation constants (K_D values).

The protein concentration to be used in STD NMR experiments depends on the molecular weight of the protein and is usually within the 10^{-4}-10^{-10} M concentration range.[53] STD experiments at different protein concentrations (8 μM, 15 μM 25 μM) were acquired before to set 8.0 μM FPPS as the concentration to be used in the full set of STD experiments. Indeed, the limit of protein concentration was imposed by the solubility of the ligands that at 1.25 mM precipitate, affecting the reliability of the results.

As a reference, we measured the K_D constants for compounds **i6A** and **2**, as previously reported [20, 30] and corresponding to ~1.0 mM and ~0.19 mM, respectively. Subsequently, STD-NMR experiments were collected for each compound **2a-m** (Figures S15-S28, see Supplementary Information). NMR samples containing 8.0 μM FPPS were titrated with compounds **2a-m** to build-up STD at protein-ligand molar ratios of 1:10, 1:20, 1:30, 1:50, 1:70, and 1:100. For each titration point, STD experiments were acquired using different saturation times (0.50, 1.00, 1.50, 2.00, 3.00, 4.00, and 5.00 s).[54] Compound **2f**, characterized by the *p*-tertbutylphenyl ring in the N6 position of adenosine, showed the most significant STD effect, with a 30% decrease in the intensity of the signals from the *p*-tertbutyl protons (Figure 5). For this compound, we quantitatively evaluated the STD data to calculate the K_D for the FPPS/**2f** complex. We collected data from experiments at different protein-ligand ratios and saturation time conditions, according to the methodology developed by *Angulo et al.*[54] The mean K_D value calculated for the single protons of **2f** was ~0.14 mM (Table 2).

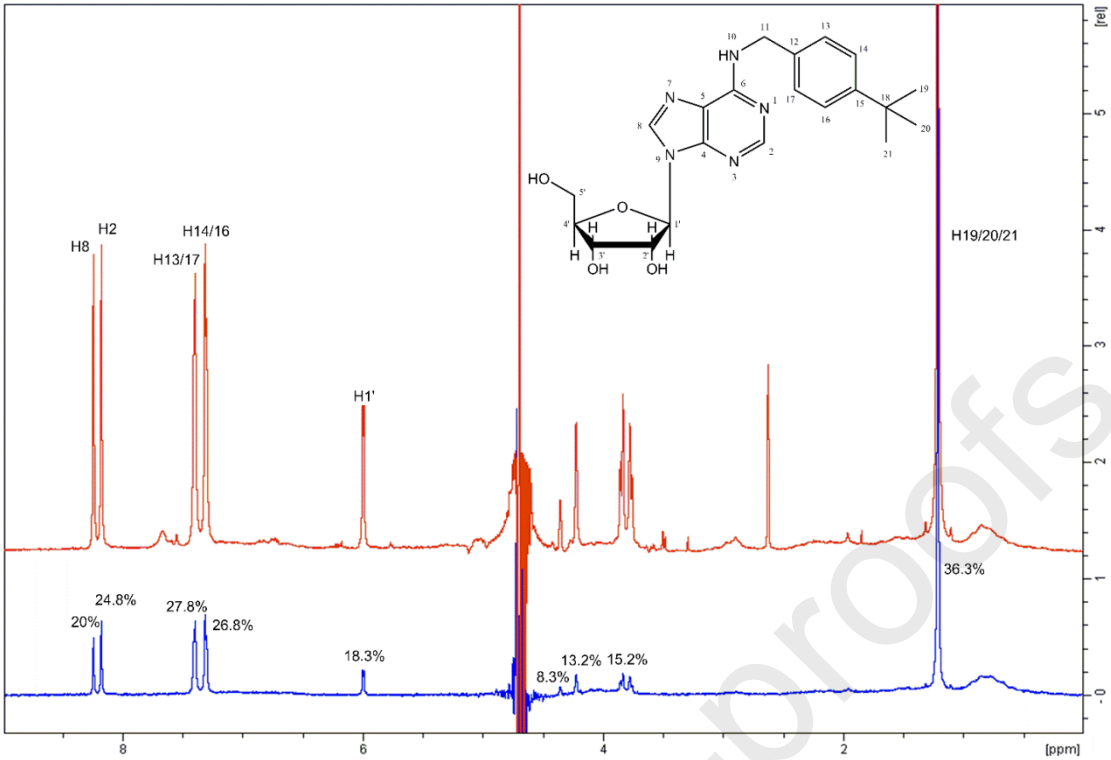

Figure 5. STD-NMR spectra of FPPS/**2f**, 1:100 molar ratio. Red shows the off-resonance spectrum and blue shows the STD spectrum.

protein-ligand (2f) system	K_D (from STD-AF initial slope) [mM]
proton H8	0.14 ± 0.02 mM
proton H2	0.14 ± 0.01 mM
proton H13/17	0.14 ± 0.02 mM
proton H14/16	0.14 ± 0.02 mM
proton H1'	0.13 ± 0.01 mM
proton H2'	0.21 ± 0.04 mM
proton H3'	0.17 ± 0.03 mM
proton H5'	0.06 ± 0.01 mM
proton H19/20/21	0.14 ± 0.02 mM

Table 2. Dissociation constants (K_D) calculated from the isotherms of the initial growth rates of the STD-AF values of the protein-ligand systems studied herein.

These values represent an improvement in **2f**-FPPS binding compared to **2**, indicating that the introduction of the hindrance of the tertbutyl moiety in the *para* position of the benzyl ring

leads to more active FPPS ligands. To verify that the detected interaction of compound **2f** with FPPS involves the active site instead of an allosteric site, we titrated the FPPS-**2f** complex with increasing concentrations of the FPPS allosteric modulator 5,7-dichloro-3-(carboxymethyl)-1H-indole-2-carboxylic acid (IC_{50} ~6 μM)[18, 55] following the procedure previously described.[20] Notably, 80 μM Zol, a known high-affinity active site FPPS inhibitor, induced observable variations in the FPPS-**2f** STD spectrum.

2.4 ^{1}H-NMR enzymatic assay

The screening of new FPPS inhibitors is generally based on the measurement of enzymatic activity via a radio-enzymatic test.[56] To avoid experiments that use ^{31}P radioligands, a new enzymatic assay was developed by employing NMR quantitative analysis. The proposed methodology includes the quantification of the FPPS-catalysed reaction rate by measuring the variation of the signal intensities of FPPS substrates IPP/DMAPP *vs.* the product GPP. The real-time enzyme kinetics of the substrates DMAPP and IPP converting to the product GPP by FPPS is shown in Figure 6a. In a preliminary step, we set up the procedure by determining the exact concentrations of the substrates (DMAPP and IPP) and FPPS enzyme to be used to obtain the valuable IC_{50} values for FPPS ligands (*vide infra,* Methods). Accordingly, ^{1}H-NMR experiments were recorded on samples containing 200 μM DMAPP, 400 μM IPP, and 8 μM FPPS enzyme at 310 K. As seen in Figure 6a, by the end of the experiment, the DMAPP (**S_1**) (5.53 ppm; 3.58 ppm; 1.80 ppm) and IPP (S_2) (4.14 ppm; 2.47 ppm; 1.85 ppm) resonances converted into that of the GPP (**P**) molecule (~30 min). To prove that the ability of the synthesized compounds to bind FPPS (according to STD NMR effects) would correspond to their ability to inhibit FPPS enzymatic activity, the conversion of substrates DMAPP (**S_1**) and IPP (**S_2**) was monitored in the presence of FPPS and compounds **2** (Figure S29, see

Supplementary Information) and **2f**. Figure 6b shows that at time T=30 min, the GPP signals were 4% of the corresponding signals recorded in the absence of compound **2f**.

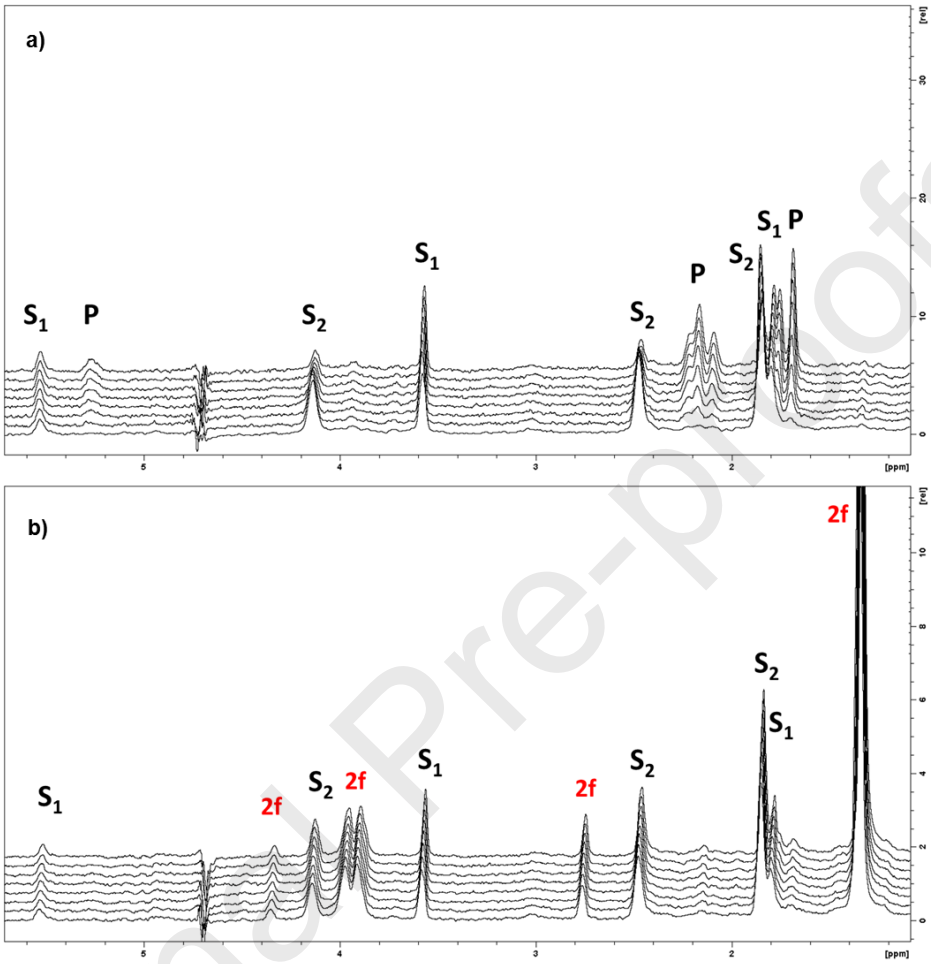

Figure 6. Real-time ^{1}H-NMR spectra of the enzyme kinetics on a Bruker 600 MHz spectrometer. **a)** The conversion of 400 µM IPP (**S_2**) and 200 µM DMAPP (**S_1**) produces GPP (**P**); **b)** GPP (**P**) production was inhibited by the addition of 1 mM **2f.**

To calculate IC_{50} values for **2** and **2f**, the ^{1}H-NMR spectra of IPP and DMAPP in the presence of FPPS were recorded at different concentrations of **2** (1 mM, 1.4 mM, 1.8 mM and 2 mM) and **2f** (0.5 mM, 0.65 mM, 0.85 mM and 1 mM). By plotting the reaction rate at the given inhibitor concentration *vs.* our inhibitor concentration, IC_{50} values of ~ 6.10 mM and ~1.18 mM were calculated for **2** and **2f**, respectively (GraphPad Prism)[57] (Figure 7a-b). An

orthogonal colorimetric assay, as previously described, validated the calculated IC_{50} and K_D values (Figure S31, see Supplementary Information).[58]

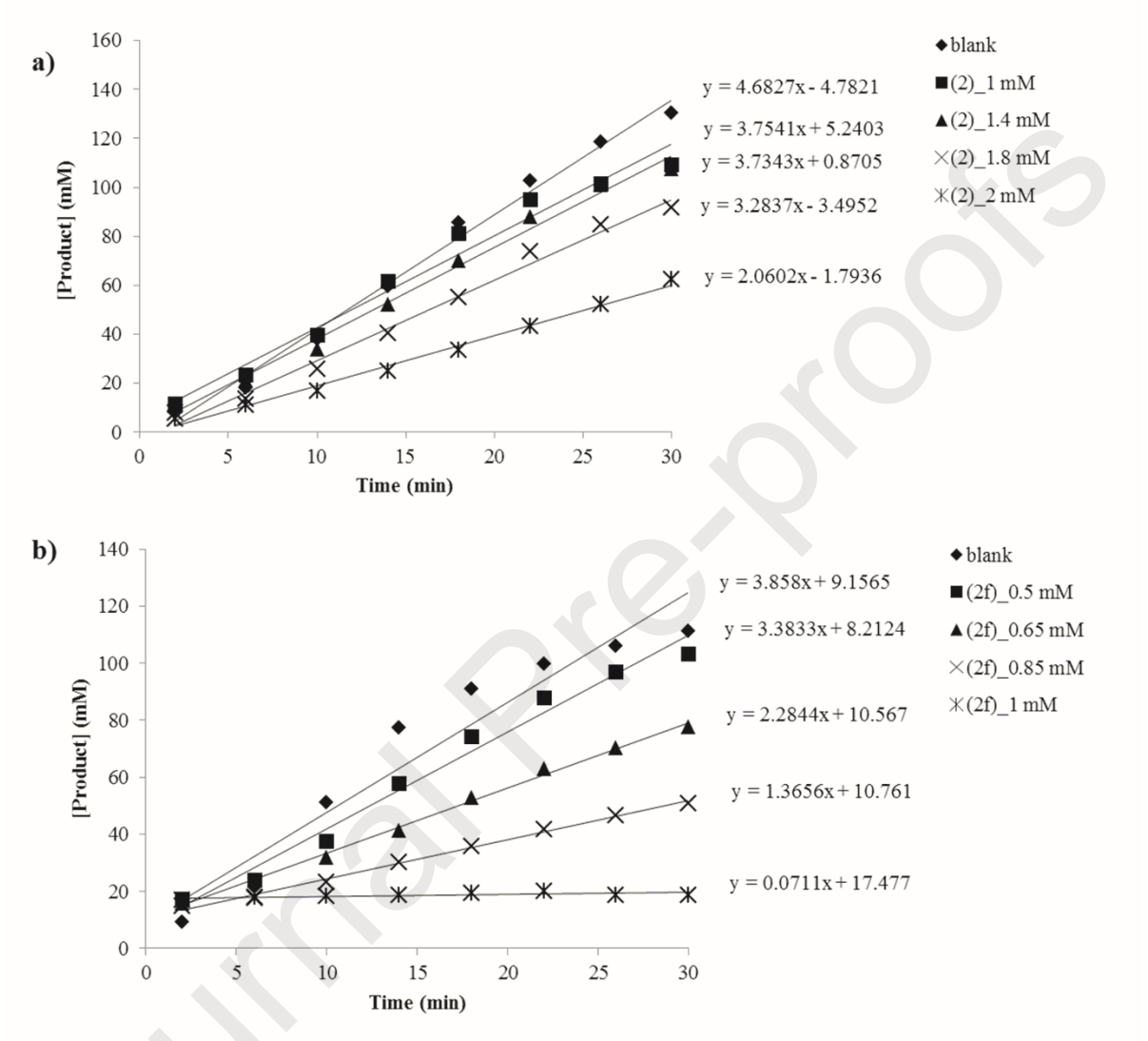

Figure 7. Variation of GPP concentration *vs.* time (min) in the presence of **a) 2** and **b) 2f**. From the maximum slope, which was achieved within approximately 30 min, the trend lines were generated with their associated equations.

3. Biological activity

3.1 Cell viability of N6-benzyladenosine analogues

Since compound **2** showed significant activity in inhibiting glioma cell growth,[30] the effects of **2a-m** were investigated by the BrdU incorporation assay. Along with all the compounds

tested, **i6A** and **2** were used as reference compounds in a 0.3-20 µM concentration range on proliferating U87MG cells. The data reported in Figure 8 show that even though no compound reached the same cytostatic efficacy of **2**, compounds **2c, 2d, 2h,** and **2i** exert significant cytotoxic activity. This result is consistent with the presence of halogen atoms (for **2c, 2d, 2h**) and a nitro moiety (for **2i**) in the *para* position of the benzyl ring. Among the compounds showing significant cytotoxicity, compounds **2a** and to a greater extent, **2c**, maintained discrete dose-dependent inhibition of proliferation compared to untreated cells (Figure 8).

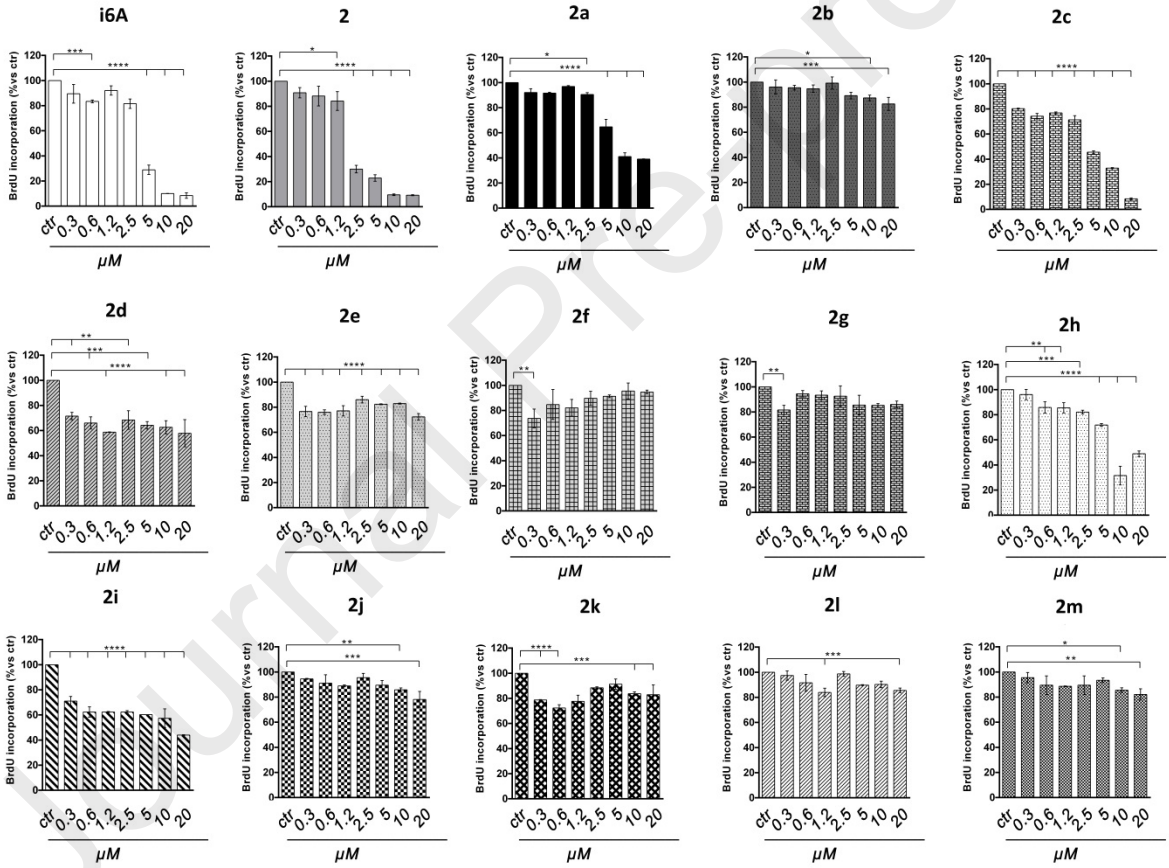

Figure 8. Effect of analogues **2** on cellular proliferation of the U87MG human glioma cell line. U87MG cells were cultured for 48 h in the presence of the indicated concentrations (0–20 µM) of **i6A**, **2** and **2**(**a-m**) before the analysis of cell proliferation by the BrdU incorporation assay. The results are representative of three independent experiments performed in triplicate and expressed as the mean ± SD (ANOVA, *p<0.05, **p<0.01 and ***p<0.001).

3.2 Immunostimulatory activity of N6-benzyladenosine analogues

As the inhibition of FPPS achieved by amino bisphosphonates stimulates Vγ9Vδ2 T-cell expansion among peripheral blood lymphocytes,[13, 14] we tested the γδ T cell-stimulating ability of the various compounds in primary PBMC cultures. Freshly isolated PBMCs from healthy donors were incubated for 14 days with **i6A**, **2** and **2a-m** stimuli in the presence of suboptimal doses of IL-2. Zol and IPP accumulated in antigen-presenting cells (APCs) and immunostimulatory phosphoantigens for γδ T cells were used as references. When γδ T cells were efficiently stimulated, they formed clusters on day 5. As expected, clusters and aggregates of γδ T cells can be observed when the PBMCs were successfully stimulated with Zol and IPP (Figure 9a).

In contrast, no clusters or aggregates were observed when the growth of γδ T cells was not adequate (in medium in the absence of IL-2 or IL-2 alone). Interestingly, **2i, 2h, 2f,** and **2a** showed an in vitro stimulatory profile that was similar or improved compared to that achieved by the bisphosphonate Zol (Figure 9b). Furthermore, flow cytometric determination of the percent of γδ T cells after 14 days showed that compounds **2a-m** generally induced toxicity comparable to Zol; however, these toxicity values were lower than reference compound **2** (Figure 9c).

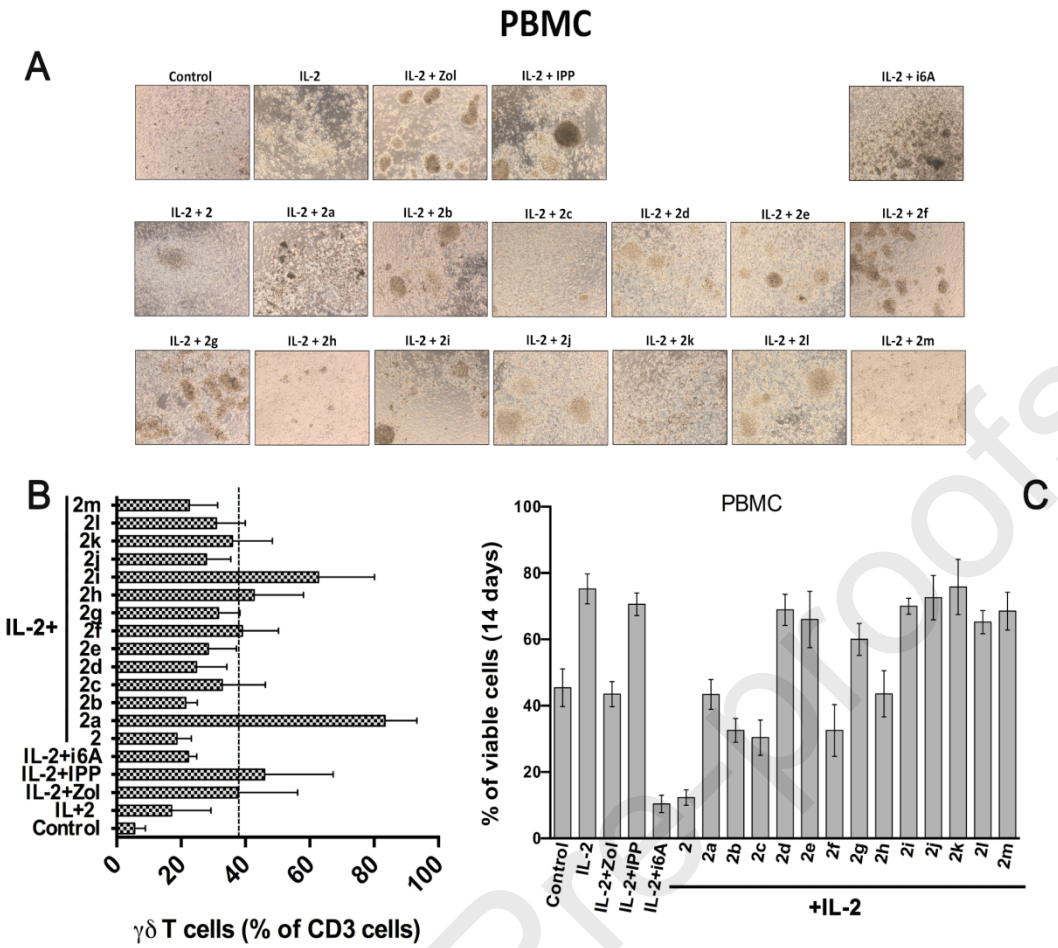

Figure 9. A selective outgrowth of γδ T cells upon stimulation with analogues **2**. **a)** PBMCs were stimulated with human IL-2 (IL-2), zoledronic acid (Zol), IPP or compounds (**i6A**, **2**, **2a-m**) to final concentrations of 150 IU/ml for IL-2 and 5 μM for all others. Cells were imaged by brightfield microscopy. Representative fields are shown. Clusters and aggregates of γδ T cells can be observed on day 7, when γδ T cells, following treatments, were successfully expanded. **b)** Determination of the percentage of γδ T cells as evaluated by flow cytometric analysis on day 14. Histograms report the percent ± SD of CD3+γδ+ positive cells compared to the total PBMC population. **c)** At the end of cell culture, the viability of the stimulated PBMCs was examined by propidium iodide (PI) staining and flow cytometry analysis. Histograms report the percent ± SD of PI-negative viable cells in all conditions tested.

4. Discussion

The search for new anticancer FPPS inhibitors that can overcome the pharmacokinetic limits of N-BPs has currently received increasing interest.[15-17] In the present contribution, we

report an NMR screening of new ligands of FPPS designed and synthesized starting from the N6-benzyladenosine scaffold.

N6-isopentenyladenosine (**i6A**) and N6-benzyladenosine (**2**) are modified nucleosides belonging to the cytokine family.[21, 24, 43] They control many processes in plants and exert in *vitro* and *in vivo* cytostatic and pro-apoptotic activities[4] through a mechanism related to the inhibition of FPPS expression and activity.[32] Based on *in silico* inverse virtual screening and NMR experiments, we showed that the biological activities of **i6A** and **2** depend, at least in part, on the direct inhibition of FPPS catalytic activity. Computational data and NMR experiments provided the structural requirements governing the interaction between the compounds and FPPS.[20, 30]

Many structural models of FPPS are available in the PDB (https://www.rcsb.org/; https://www.uniprot.org/uniprot/P14324). All these models agree on the FPPS catalytic site characterized by i) an allylic sub-pocket (DMAPP/GPP binding site) including two Asp-rich motifs that bind the pyrophosphate moiety of DMAPP/GPP *via* Mg^{2+} cation interactions and ii) a basic region rich in Arg residues that binds IPP through salt-bridge interactions. By docking **i6A** and **2** in the FPPS binding pocket (ID code: 5YGI), we observed that in the most representative binding poses (Figure 3), i) the riboside sugar and the adenine ring occupy the DMAPP sub-pocket through electrostatic interactions with Mg^{2+} ions and conserved Asp residues and ii) the benzyl ring occupies a large hydrophobic cavity capable of accommodating new bulky chemical moieties. In agreement with these structural requirements, compounds **2a-m**, including chemical substituents characterized by different degrees of steric hindrance in the *para* position of the benzyl ring, were synthesized and tested for their ability to bind FPPS using STD-NMR experiments. Compound **2f**, the compound with a tertbutyl moiety, showed the lowest K_D value of ~0.14 mM, corresponding to an 8-fold and 2-fold increase in FPPS binding compared to **i6A** and **2**, respectively.

The activity of FPPS inhibitors has long been measured using ^{31}P radioligands.[56] More recently, LC/MS/MS FPPS inhibition assays have been developed.[18, 19] To measure the IC_{50} of **i6A** and **2**, (IC_{50} **i6A** ~1 mM and IC_{50} **2** ~0.25 mM) we used in our previous work a colorimetric assay[58] that unfortunately suffers from poor accuracy and sensitivity. To overcome these limits and to avoid the drawbacks related to the handling of the ^{31}P radioligand, we herein report a newly developed NMR enzymatic assay based on the quantitative evaluation of the ^{1}H signal intensity of FPPS substrates IPP/DMAPP *vs.* ^{1}H signal intensity of the product GPP. By applying the law of Michaelis and Menten and its derivations, we obtained IC_{50} values of ~6.10 mM and ~1.18 mM for **2** and **2f**, respectively, confirming the increased binding potency observed from the K_D values. The calculated IC_{50} values were cross validated using the previously described colorimetric assay (see Figure S31 in the Supplementary Information).

N-BPs are the only commercially available FPPS inhibitors; they bind to the allylic sub-pocket mimicking the pyrophosphate moiety of DMAPP/GPP.[7-9, 32] Because of their highly charged nature and affinity for skeletal tissue, these drugs are limited to the treatment of bone-related disorders such as osteoporosis and tumour-induced osteolytic metastases.[10]

The recent discovery of an FPPS allosteric pocket as a potential target of N-BP compounds has fuelled the search for new FPPS inhibitors to overcome the pharmacokinetic limits of bisphosphonate and become useful in broader therapeutic applications.[18, 19] As a result, several non-bisphosphonate allosteric ligands have been identified, some of which show chameleon-like behaviour, with mixed binding to both the catalytic and allosteric sites.[59-61] Very recently, the X-ray structure of FPPS co-crystallized with 6-tolylthienopyrimidine (IC_{50} 0.86 μM) highlighted the possibility of efficacious interactions at the FPPS binding site, mainly based on consistent π-π stacking interactions and excluding the participation of the phosphonate moiety.[16] NMR data and molecular docking calculations show that compounds **2a-m** in the FPPS catalytic pocket have an orientation similar to that observed in the crystal

structure of FPPS co-crystallized with 6-tolylthienopyrimidine. The sugar and adenine ring occupy the DMAPP sub-pocket, interacting with the Mg^{2+} ion and Asp residues of the conserved aspartate-rich motif.[17, 34, 35] The *p*-tertbutyl benzyl ring occupies a large hydrophobic region that engages in π-π stacking interactions with aromatic residues (F98, F99, Y204). Although the IC_{50} and the K_D values of **2** and **2f** have, at the moment, modest relevance from a drug-design perspective, the biological activity of **2** and **2f** confirms that there are many unexploited possibilities to identify new potent N-BP FPPS inhibitors, and in this way, N6-substituted adenosine derivatives can be considered promising chemical scaffolds to be further investigated.

Data collected on glioma cells indicated that **2a-m** exerts cytostatic activity in the concentration range of 10-20 μM, whereas **2** and **2f** bind and inhibit FPPS at mM concentration values. On the other hand, structure-activity relationship analysis indicates that the structural requirements governing **2a-m** cell cytotoxicity are different from those governing the interaction with the FPPS enzyme. This discrepancy between the potency of the compounds in binding to and inhibiting FPPS and the potency exhibited in a more complex cellular model was already evident in our previous investigation. Here, the high efficiency of **2** to inhibit glioma cell growth through cholesterol depletion provided a clear indication that **2** affects the MVA metabolic pathway. However, even in this case, **2** showed greater effectiveness in cultured cells compared to the in vitro FPPS assay. Thus, the previous and presently reported data support the hypothesis that FPPS might not be the only target of the benzyladenosine compounds, and other key enzymes and intermediate metabolites of the mevalonate and isoprenoid pathways can be affected by their action.[62]

Increasing evidence has shown that inhibition of FPPS using N-BPs induces IPP accumulation, and this, in turn, activates γδ T cells.[13] Monocytes that accumulate IPP become APC and stimulate Vγ9Vδ2 T cells in the peripheral blood.[63] Therefore, blocking the mevalonate

pathway through the inhibition of FPPS has a final immunostimulatory effect. Therefore, immunotherapy based on the combinatorial use of both IL-2 and Zol for the expansion of γδ T cells has become a widely used approach in several cancer treatments.[14] To investigate the ability of compounds **2a-m** to affect the action of enzymes and intermediate metabolites in the mevalonate and isoprenoid pathways, we measured the ability of compounds **2a-m** to induce expansion of γδ T cell cultures analogous to that achieved by interleukin-2 (IL-2) plus Zol,[11] with N-BP used as control. As observed in Figure 9, **2a**, **2f**, **2h**, and **2i** exhibited an in vitro stimulatory profile that was similar or improved compared to that achieved by Zol (Figure 9b); analysis of γδ T cell viability after 14 days showed that these compounds induce toxicity comparable to Zol; however, their effects were lower than that of **2**.

Taken together, our data provide evidence that N6-benzyladenosine derivatives may play a role similar to N-BPs in interacting with FPPS and thus interfering with the mevalonate pathway. Therefore, these derivatives represent a good chemical scaffold to be further investigated for the development of N-BP FPPS inhibitors, allowing the *ex vivo* expansion of cytotoxic cells to be used in adoptive immunotherapy with a synergistic, discrete, cytostatic ability.

5. Methods

5.1 Molecular docking

AutoDock Vina (version 1.1.2)[36] was used for all docking calculations. The starting conformations for docking studies of analogues **2** were built with Maestro (version 9.6).[64] Three-dimensional models of each compound for the subsequent docking calculations were preliminary optimized by the conjugate gradient (0.05 Å convergence threshold). After optimization of the analogues, molecular charges were calculated by the Gasteiger-Marsili method. Finally, the 3D structures were saved in .pdbqt format for molecular docking studies. The 3D FPPS protein model was obtained from the Protein Data Bank database (PDB ID:

5YGI).[35] Water molecules were removed, and the obtained file was then processed with AutoDock Tools 1.5.6, merging non-polar hydrogens and adding Gasteiger charges. For all docked ligands, all bonds were considered rotatable. For an exhaustive exploration of conformational space, all runs were performed with 300 iterations yielding 20 structures. For all docking calculations, a grid box size of 26.51 Å (x, y, and z) was used and centred on the target binding site (spatial coordinates: -16.92 x, 29.55 y, -9.78 z). The resulting data with the most favourable free energies of binding were analysed. All 3D models were depicted using Maestro 9.6.[64]

5.2 Chemistry

All reagents were purchased from Sigma-Aldrich (Milan, Italy) in the highest available purity and were used as received. All reactions involving air or moisture-sensitive reagents were carried out in a dry nitrogen atmosphere using freshly distilled solvents. DCM, CH_3CN, and methanol were distilled from CaH_2. Dry DMF was purchased and used without further distillation. When necessary, compounds were dried *in vacuo* over P_2O_5 or by the azeotropic removal of water with toluene under reduced pressure. All MW reactions were conducted in a CEM Explorer apparatus under monomode irradiation. Reaction temperatures were measured externally; reactions were monitored by thin-layer chromatography (TLC) on Merck silica gel plates (0.25 mm) and visualized by UV light, $KMnO_4$, *p*-anisaldehyde, or ninhydrin solutions and drying. Flash chromatography was performed on Merck silica gel 60 (particle size: 0.040-0.063 mm), and the solvents employed were of analytical grade. Yields refer to chromatographically and spectroscopically (^{1}H- and ^{13}C-NMR) pure compounds. Silica gel (grade 60 PF254) was used for preparative TLC (PTLC). NMR spectra were generally recorded at room temperature on Bruker Avance series 400 and 600 MHz spectrometers. Chemical shifts (δ) are reported in ppm relative to the residual solvent peak ($CHCl_3$, δ: 7.26, $^{13}CDCl_3$, δ: 77.0;

CD_2HOD, δ: 3.35, $^{13}CD_3OD$, δ: 49.0), and the multiplicity of each signal is designated by the following abbreviations: s, singlet; d, doublet; t, triplet; q, quartet; m, multiplet; br, broad; app, apparent. Coupling constants (J) are quoted in Hz. High-resolution mass spectra (HRMS) were recorded on a high-resolution mass spectrometer equipped with electrospray (ESI) and nanospray sources, a quadrupole-time of flight hybrid analyser coupled with capillary UPLC system (Q-TOF Premier/nanoAquity, Waters) in positive mode, and protonated molecular ions $[M+H]^+$ were used for empirical formula confirmation. Liquid chromatography was performed on a Waters system (Milford, Massachusetts, USA) consisting of a Waters 486 tunable absorbance detector and a Varian 9012 pump. Samples were prepared by dissolving compounds **2a-m** in methanol (0.5 mg/mL) at 0.2 mL/min. The injection volume was 10 µL. Compounds **2a-m** were analysed on a Symmetry® (C18 column (4.6 × 250 mm, 5 µm) under gradient elution at a flow rate of 0.9 mL/min. The mobile phases consisted of 2% (v/v) acetic acid in water (solvent A) and 2% (v/v) acetic acid in acetonitrile (solvent B). The following gradient was used: 0–20 min 10–90% B, 20–24 min 90–10% B, and return to the initial conditions over 3 min. UV detection was obtained at λ = 254 nm (Figure S30, See Supplementary Information).

General procedure for the solvent free MW synthesis of N6-benzyladenosine derivatives 2a-m. Synthesis of (2R, 3R, 4S, 5R)-2-(6-(benzylamino)-9H-purin-9-yl)-5-(hydroxymethyl) tetrahydrofuran-3,4-diol, **2**. In a 7 mL MW vessel, 6-chloropurinoriboside **3** (20 mg, 0.07 mmol), benzylamine 4 (7.5 mg, 0.07 mmol, 7.7 µL) and triethylamine (7.08 mg, 0.07 mmol, 9.8 µL) were mixed. The solid mixture was stirred in CEM Explorer®. MW Method: T = 210 °C, Power: 300 W, Hold Time: 1 min, P = 250 PSI, Power Max activated. After cooling, the solvent was removed *in vacuo* and the crude was dissolved in methanol and then purified on PTLC (DCM/MeOH 9:1) to afford compound **2** as white solid (24 mg, 94%). ^{1}H-NMR (600

MHz, MeOD) δ 8.30 (s, 1H), 8.28 (s, 1H), 7.43 (d, *J* = 7.5 Hz, 2H), 7.36 (t, *J* = 7.6 Hz, 2H), 7.29 (t, *J* = 7.3 Hz, 1H), 6.01 (d, *J* = 6.4 Hz, 1H), 4.82 – 4.77 (m, 1H), 4.37 (dd, *J* = 4.9, 2.5 Hz, 1H), 4.22 (d, *J* = 2.4 Hz, 1H), 3.93 (dd, *J* = 12.5, 2.3 Hz, 1H), 3.79 (dd, *J* = 12.5, 2.5 Hz, 1H) ppm. HRMS (ESI-Q-TOF) m/z [M + H]+ Calcd. for $C_{17}H_{20}N_5O_4$: 358.1510; Found 358.1515. Rt: 8.92 min.

Synthesis of (2*R*,3*S*,4*R*,5*R*)-2-(hydroxymethyl)-5-(6-((3-methylbenzyl)amino)-9*H*-purin-9-yl)tetrahydrofuran-3,4-diol, **2a**. Compound **2a** was obtained as a white solid (24 mg, 92%) by following general procedure for the solvent free MW synthesis of N6-benzyladenosine derivatives by using 6-chloropurinoriboside **3** (20 mg, 0.07 mmol) 3-methylbenzylamine **4a** (8.48 mg, 0.07 mmol, 8.8 µL) and triethylamine (7.08 mg, 0.07 mmol, 9.8 µL). ^{1}H-NMR (600 MHz, MeOD) δ 8.29 (d, *J* = 10.4 Hz, 2H), 7.22 (dd, *J* = 19.2, 9.3 Hz, 3H), 7.11 (d, *J* = 7.1 Hz, 1H), 6.01 (d, *J* = 6.3 Hz, 1H), 4.80 (dd, *J* = 13.0, 7.1 Hz, 3H), 4.39 – 4.36 (m, 1H), 4.22 (s, 1H), 3.93 (d, *J* = 12.5 Hz, 1H), 3.79 (d, *J* = 12.5 Hz, 1H) ppm. HRMS (ESI-Q-TOF) m/z [M + H]+ Calcd. for $C_{18}H_{22}N_5O_4$: 372.1666; Found 372.1659. Rt: 9.59 min.

Synthesis of (2*R*,3*R*,4*S*,5*R*)-2-(6-(([1,1'-biphenyl]-3-ylmethyl)amino)-9*H*-purin-9-yl)-5-(hydroxymethyl)tetrahydrofuran-3,4-diol, **2b**. Compound **2b** was obtained as a white solid (27 mg, 89%) by following general procedure for the solvent free MW synthesis of N6-benzyladenosine derivatives by using 6-chloropurinoriboside **3** (20 mg, 0.07 mmol),3-phenylbenzylamine **4b** (14.66 mg, 0.07 mmol) and triethylamine (7.08 mg, 0.07 mmol, 9.8 µL). ^{1}H-NMR (600 MHz, MeOD) δ 8.31 (s, 2H), 7.70 (s, 1H), 7.63 (d, *J* = 7.5 Hz, 2H), 7.55 (d, *J* = 7.2 Hz, 1H), 7.44 (dt, *J* = 18.8, 7.2 Hz, 4H), 7.36 (t, *J* = 7.2 Hz, 1H), 6.01 (d, *J* = 6.3 Hz, 1H), 4.80 (t, *J* = 5.6 Hz, 1H), 4.39 – 4.35 (m, 1H), 4.22 (s, 1H), 3.93 (d, *J* = 12.5 Hz, 1H), 3.79 (d, *J* = 12.5 Hz, 1H) ppm. HRMS (ESI-Q-TOF) m/z [M + H]+ Calcd. for $C_{23}H_{24}N_5O_4$: 434.1823; Found 434.1829. Rt: 12.19 min.

Synthesis of (2*R*,3*R*,4*S*,5*R*)-2-(6-((4-fluorobenzyl)amino)-9*H*-purin-9-yl)-5-(hydroxymethyl)tetrahydrofuran-3,4-diol, **2c**. Compound **2c** was obtained as a white solid (24 mg, 92%) by following general procedure for the solvent free MW synthesis of N6-benzyladenosine derivatives by using 6-chloropurinoriboside **3** (20 mg, 0.07 mmol), 4-fluoro-benzylamine **4c** (8.76mg, 0.07mmol, 8.0µL) and triethylamine (7.08 mg, 0.07 mmol, 9.8 µL). ^{1}H-NMR (600 MHz, MeOD) δ 8.29 (d, *J* = 9.8 Hz, 4H), 7.45 (dd, *J* = 7.9, 5.7 Hz, 4H), 7.08 (t, *J* = 8.7 Hz, 4H), 6.00 (d, *J* = 6.4 Hz, 2H), 4.81 – 4.77 (m, 3H), 4.37 (dd, *J* = 4.7, 2.3 Hz, 2H), 4.21 (d, *J* = 2.1 Hz, 2H), 3.93 (dd, *J* = 12.5, 2.0 Hz, 2H), 3.79 (dd, *J* = 12.5, 2.2 Hz, 2H) ppm. HRMS (ESI-Q-TOF) m/z [M + H]+ Calcd. for $C_{17}H_{19}N_5O_4$: 376.1416; Found 376.1411. Rt: 9.00 min.

Synthesis of (2*R*,3*R*,4*S*,5*R*)-2-(6-((4-bromobenzyl)amino)-9*H*-purin-9-yl)-5-(hydroxymethyl)tetrahydrofuran-3,4-diol, **2d**. Compound **2d** was obtained as a white solid (27 mg, 88%) by following general procedure for the solvent free MW synthesis of N6-benzyladenosine derivatives by using 6-chloropurinoriboside **3** (20 mg, 0.07 mmol), 4-bromo-benzylamine **4d** (13.0 mg, 0.07 mmol) and triethylamine (7.08 mg, 0.07 mmol, 9.8 µL). ^{1}H-NMR (600 MHz, MeOD) δ 8.32 (d, *J* = 13.8 Hz, 2H), 7.53 (d, *J* = 7.8 Hz, 2H), 7.38 (d, *J* = 7.7 Hz, 2H), 6.03 (d, *J* = 5.9 Hz, 1H), 4.82 (d, *J* = 5.4 Hz, 2H), 4.39 (s, 1H), 4.24 (s, 1H), 3.96 (d, *J* = 12.5 Hz, 1H), 3.82 (d, *J* = 12.5 Hz, 1H) ppm. HRMS (ESI-Q-TOF) m/z [M + H]+ Calcd. for $C_{17}H_{19}BrN_5O_4$: 436.0615; Found 436.0611. Rt: 10.53 min.

Synthesis of (2*R*,3*S*,4*R*,5*R*)-2-(hydroxymethyl)-5-(6-((4-methylbenzyl)amino)-9*H*-purin-9-yl)tetrahydrofuran-3,4-diol, **2e**. Compound **2e** was obtained as a white solid (23 mg, 89%) by following general procedure for the solvent free MW synthesis of N6-benzyladenosine derivatives by using 6-chloropurinoriboside **3** (20 mg, 0.07 mmol), 4-methyl-benzylamine **4e** (8.5 mg, 0.07 mmol, 9.0 µL) and triethylamine (7.08 mg, 0.07 mmol, 9.8 µL). ^{1}H-NMR (600 MHz, MeOD) δ 8.15 (d, *J* = 18.7 Hz, 2H), 7.15 (d, *J* = 7.7 Hz, 2H), 7.03 (d, *J* = 7.5 Hz, 2H),

5.85 (d, *J* = 6.5 Hz, 1H), 4.64 (t, *J* = 5.4 Hz, 3H), 4.21 (d, *J* = 2.8 Hz, 1H), 4.06 (s, 1H), 3.78 (d, *J* = 11.6 Hz, 1H), 3.64 (d, *J* = 11.3 Hz, 1H) ppm. HRMS (ESI-Q-TOF) m/z [M + H]+ Calcd. for $C_{18}H_{22}N_5O_4$: 372.1666; Found 372.1661. Rt: 9.73 min.

Synthesis of (2*R*,3*R*,4*S*,5*R*)-2-(6-((4-(*tert*-butyl)benzyl)amino)-9*H*-purin-9-yl)-5-(hydroxymethyl)tetrahydrofuran-3,4-diol, **2f**. Compound **2f** was obtained as a white solid (26 mg, 91%) by following general procedure for the solvent free MW synthesis of N6-benzyladenosine derivatives by using 6-chloropurinoriboside **3** (20 mg, 0.07 mmol), 4-tert-butyl-benzylamine **4f** (17.13 mg, 0.07 mmol) and triethylamine (7.08 mg, 0.07 mmol, 9.8 µL). ^{1}H-NMR (600 MHz, MeOD) δ 8.29 (d, *J* = 7.6 Hz, 2H), 7.41 (d, *J* = 7.9 Hz, 2H), 7.35 (d, *J* = 8.0 Hz, 2H), 6.00 (d, *J* = 6.3 Hz, 1H), 4.81 – 4.77 (m, 2H), 4.39 – 4.34 (m, 1H), 4.21 (s, 1H), 3.93 (d, *J* = 12.5 Hz, 1H), 3.79 (d, *J* = 12.5 Hz, 1H) ppm. HRMS (ESI-Q-TOF) m/z [M + H]+ Calcd. for $C_{21}H_{28}N_5O_4$: 414.2136; Found 414.2140. Rt: 12.61 min.

Synthesis of (2*R*,3*S*,4*R*,5*R*)-2-(hydroxymethyl)-5-(6-((quinolin-2-ylmethyl)amino)-9*H*-purin-9-yl)tetrahydrofuran-3,4-diol, **2g**. Compound **2g** was obtained as a white solid (25 mg, 87%) by following general procedure for the solvent free MW synthesis of N6-benzyladenosine derivatives by using 6-chloropurinoriboside **3** (20 mg, 0.07 mmol), 2-Quinolinemethanamine **4g** (11.07 mg, 0.07 mmol) and triethylamine (7.08 mg, 0.07 mmol, 9.8 µL). ^{1}H-NMR (600 MHz, MeOD) δ 8.33 (dd, *J* = 22.2, 13.7 Hz, 9H), 8.10 (d, *J* = 8.5 Hz, 3H), 7.95 (d, *J* = 8.1 Hz, 3H), 7.80 (t, *J* = 7.6 Hz, 3H), 7.61 (dd, *J* = 16.0, 8.1 Hz, 6H), 6.03 (d, *J* = 6.3 Hz, 3H), 4.81 (t, *J* = 5.6 Hz, 4H), 4.38 (d, *J* = 2.3 Hz, 3H), 4.22 (s, 4H), 3.93 (d, *J* = 12.4 Hz, 4H), 3.81 (dd, *J* = 19.7, 12.5 Hz, 4H) ppm. HRMS (ESI-Q-TOF) m/z [M + H]+ Calcd. for $C_{20}H_{21}N_6O_4$: 409.1619; Found 409.1612. Rt: 6.93 min.

Synthesis of (2*R*,3*R*,4*S*,5*R*)-2-(6-((4-chlorobenzyl)amino)-9*H*-purin-9-yl)-5-(hydroxymethyl)tetrahydrofuran-3,4-diol, **2h**. Compound **2h** was obtained as a white solid (25 mg, 90%) by following general procedure for the solvent free MW synthesis of N6-

benzyladenosine derivatives by using 6-chloropurinoriboside **3** (20 mg, 0.07 mmol), 4-chloro-benzylamine **4h** (9.9 mg, 0.07 mmol, 8.85 µL) and triethylamine (7.08 mg, 0.07 mmol, 9.8 µL). ^{1}H-NMR (600 MHz, MeOD) δ 8.29 (d, *J* = 15.4 Hz, 2H), 7.42 (d, *J* = 8.3 Hz, 2H), 7.36 (d, *J* = 8.4 Hz, 2H), 6.00 (d, *J* = 6.4 Hz, 1H), 4.81 – 4.77 (m, 1H), 4.37 (dd, *J* = 5.0, 2.5 Hz, 1H), 4.21 (d, *J* = 2.4 Hz, 1H), 3.93 (dd, *J* = 12.5, 2.3 Hz, 1H), 3.79 (dd, *J* = 12.5, 2.5 Hz, 1H) ppm. HRMS (ESI-Q-TOF) m/z [M + H]+ Calcd. for $C_{17}H_{19}ClN_5O_4$: 392.1120; Found 392.1127. Rt: 10.34 min.

Synthesis of (2R,3S,4R,5R)-2-(hydroxymethyl)-5-(6-((4-nitrobenzyl)amino)-9H-purin-9-yl)tetrahydrofuran-3,4-diol, **2i**. Compound **2i** was obtained as a white solid (27 mg, 88%) by following general procedure for the solvent free MW synthesis of N6-benzyladenosine derivatives by using 6-chloropurinoriboside **3** (20 mg, 0.07 mmol), 4-nitro-benzylamine **4i** (13.20 mg, 0.07 mmol) and triethylamine (7.08 mg, 0.07 mmol, 9.8 µL). ^{1}H-NMR (600 MHz, MeOD) δ 8.33 (s, 1H), 8.28 (s, 1H), 8.25 (s, 1H), 8.23 (s, 1H), 7.66 (d, *J* = 8.6 Hz, 2H), 6.01 (d, *J* = 6.4 Hz, 1H), 4.81 – 4.77 (m, 1H), 4.37 (dd, *J* = 5.0, 2.5 Hz, 1H), 4.22 (d, *J* = 2.4 Hz, 1H), 3.93 (dd, *J* = 12.5, 2.4 Hz, 1H), 3.79 (dd, *J* = 12.5, 2.6 Hz, 1H) ppm. HRMS (ESI-Q-TOF) m/z [M + H]+ Calcd. for $C_{17}H_{19}N_6O_6$: 403.1361; Found 403.1354. Rt: 8.84 min.

Synthesis of (2*R*,3*S*,4*R*,5*R*)-2-(hydroxymethyl)-5-(6-((4-methoxybenzyl)amino)-9*H*-purin-9-yl)tetrahydrofuran-3,4-diol, **2j**. Compound **2j** was obtained as a white solid (25 mg, 88%) by following general procedure for the solvent free MW synthesis of N6-benzyladenosine derivatives by using 6-chloropurinoriboside **3** (20 mg, 0.07 mmol), 4-methoxy-benzylamine **4j** (9.6 mg, 0.07 mmol, 9.3µL) and triethylamine (7.08 mg, 0.07 mmol, 9.8 µL). ^{1}H-NMR (600 MHz, MeOD) δ 8.30 (s, 2H), 7.36 (d, *J* = 8.5 Hz, 2H), 6.92 (d, *J* = 8.6 Hz, 2H), 6.00 (d, *J* = 6.4 Hz, 1H), 4.82 – 4.77 (m, 2H), 4.37 (dd, *J* = 5.0, 2.5 Hz, 1H), 4.22 (d, *J* = 2.4 Hz, 1H), 3.93 (dd, *J* = 12.5, 2.3 Hz, 1H), 3.82 (s, 3H), 3.79 (dd, *J* = 12.6, 2.6 Hz, 1H) ppm. HRMS (ESI-Q-TOF) m/z [M + H]+ Calcd. for $C_{18}H_{22}N_5O_5$: 388.1615; Found 388.1608. Rt: 8.93 min.

Synthesis of (2*R*,3*R*,4*S*,5*R*)-2-(6-((4-ethoxybenzyl)amino)-9*H*-purin-9-yl)-5-(hydroxymethyl)tetrahydrofuran-3,4-diol, **2k**. Compound **2k** was obtained as a white solid (24 mg, 84%) by following general procedure for the solvent free MW synthesis of N6-benzyladenosine derivatives by using 6-chloropurinoriboside **3** (20 mg, 0.07 mmol), 4-ethoxy-benzylamine **4k** (13.58 mg, 0.07 mmol) and triethylamine (7.08 mg, 0.07 mmol, 9.8 µL). ^{1}H-NMR (600 MHz, MeOD) δ 8.29 (s, 2H), 7.34 (d, *J* = 7.9 Hz, 2H), 6.91 (d, *J* = 7.8 Hz, 2H), 6.00 (d, *J* = 6.3 Hz, 1H), 4.81 – 4.77 (m, 2H), 4.38 – 4.35 (m, 1H), 4.21 (s, 1H), 4.05 (q, *J* = 6.8 Hz, 2H), 3.93 (d, *J* = 12.5 Hz, 1H), 3.79 (d, *J* = 12.5 Hz, 1H) ppm. HRMS (ESI-Q-TOF) m/z [M + H]+ Calcd. for $C_{19}H_{24}N_5O_5$: 402.1772; Found 402.1779. Rt: 9.66 min.

Synthesis of (2*R*,3*R*,4*S*,5*R*)-2-(6-((3,5-bis(trifluoromethyl)benzyl)amino)-9*H*-purin-9-yl)-5-(hydroxymethyl)tetrahydrofuran-3,4-diol, **2l**. Compound **2l** was obtained as a white solid (31 mg, 90%) by following general procedure for the solvent free MW synthesis of N6-benzyladenosine derivatives by using 6-chloropurinoriboside **3** (20 mg, 0.07 mmol), 3,5-bistrifluoromethyl-benzylamine **4l** (17.0 mg, 0.07 mmol) and triethylamine (7.08 mg, 0.07 mmol, 9.8 µL). ^{1}H-NMR (600 MHz, MeOD) δ 8.34 (s, 1H), 8.30 (s, 1H), 8.04 (s, 2H), 7.89 (s, 1H), 6.02 (d, *J* = 6.3 Hz, 1H), 4.80 (t, *J* = 5.6 Hz, 1H), 4.38 – 4.36 (m, 1H), 4.21 (s, 1H), 3.93 (d, *J* = 12.5 Hz, 1H), 3.79 (d, *J* = 12.5 Hz, 1H) ppm. HRMS (ESI-Q-TOF) m/z [M + H]+ Calcd. for $C_{19}H_{18}F_6N_5O_4$: 494.1257; Found 494.1263. Rt: 13.03 min.

Synthesis of (2*R*,3*R*,4*S*,5*R*)-2-(6-((3,5-dimethoxybenzyl)amino)-9*H*-purin-9-yl)-5-(hydroxymethyl)tetrahydrofuran-3,4-diol, **2m**. Compound **2m** was obtained as a white solid (26 mg, 89%) by following general procedure for the solvent free MW synthesis of N6-benzyladenosine derivatives by using 6-chloropurinoriboside **3** (20 mg, 0.07 mmol), 3,5-bismethoxy-benzylamine **4m** (11.70 mg, 0.07 mmol) and triethylamine (7.08 mg, 0.07 mmol, 9.8 µL). ^{1}H-NMR (600 MHz, MeOD) δ 8.30 (d, *J* = 12.4 Hz, 2H), 6.60 (d, *J* = 1.8 Hz, 2H), 6.42 (s, 1H), 6.01 (d, *J* = 6.4 Hz, 1H), 4.82 – 4.78 (m, 2H), 4.37 (dd, *J* = 4.9, 2.4 Hz, 1H), 4.22

(d, J = 2.3 Hz, 1H), 3.93 (dd, J = 12.5, 2.2 Hz, 1H), 3.80 (d, J = 2.5 Hz, 1H) ppm. HRMS (ESI-Q-TOF) m/z [M + H]+ Calcd. for $C_{19}H_{24}N_5O_6$: 418.1721; Found 418.1728. Rt: 9.06 min.

5.3 FPPS gene expression

The plasmid p11, transformed into BL21(DE3)-pLysS cells, was a gift from Nicola Burgess-Brown (Addgene plasmid # 39131; http://n2t.net/addgene:39131; RRID: Addgene_39131) and contained the T7/Lac promoter and ampicillin resistance. FPPS was expressed in *Escherichia coli* as a fusion protein (67−419 residues) with an N-terminal poly-histidine tail and a mutation (threonine with serine) on residue 266, with a molecular weight of 43 kDa. For expression in *E. coli*, bacterial clones were grown in 1 L of LB (Luria-Bertani) medium containing 50 µg/mL ampicillin. Cell growth was monitored spectrophotometrically by measuring the OD_{600} nm periodically. When growth achieved an OD_{600} of 0.7 at 37°C, 1 mM isopropyl-D-thiogalactoside (IPTG) was added. IPTG was purchased from Sigma-Aldrich (Italy). After 6 h of cell growth, cells were pelleted by centrifugation and re-suspended in lysis buffer (50 mL of 5% glycerol, 5 mM imidazole, 500 mM NaCl, 50 mM phosphate-buffered saline (PBS) (pH 7.5)) followed by sonication. The protein was purified with a His-Trap HP column at 1 mL/min using an AKTA purifier system; the soluble extract was applied to a nickel-chelated agarose affinity column that had been equilibrated with the same buffer. The protein was eluted from the column with elution buffer (5% glycerol, 250 mM imidazole, 500 mM NaCl, 50 mM PBS (pH 7.5)). Affinity chromatography on a nickel-chelated agarose column permitted the simple one-step protein purification. Therefore, FPPS was transferred into a Vivaspin 20 concentrator with a cut-off of 3 kDa to exchange the buffer for NMR studies.

5.4 STD-NMR experiments

STD-NMR experiments were recorded at 25°C on a Bruker AV600 MHz spectrometer at a ^{1}H resonance frequency of 600 MHz equipped with a 5 mm triple resonance $^{1}H(^{13}C/^{15}N)$, z-axis pulsed-field gradient probe head. For characterization purposes, 1D and 2D HSQC/HMBC spectra of analogues **2a-m**, samples were acquired in methanol-d_4 (MeOD) at a resolution of 16 k complex points in the time domain with 32 accumulations each (sw = 7800 Hz, d1=1 s). The FPPS protein at a concentration of 8 μM in 25 mM d-Tris, 0.5 mM $MgCl_2$ and 25 mM NaCl, pH 7.4 with 1% dimethyl sulfoxide-d6 as a co-solvent, was titrated with N6-benzyladenosine analogues **2a-m** to protein/ligand molar ratios of 1:10, 1:20, 1:30, 1:50, 1:70, and 1:100. For each addition of ligands, STD build-up experiments were conducted using different saturation times (0.50, 1.00, 1.50, 2.00, 3.00, 4.00, and 5.00 s and different relaxation delays of 1.50, 2.00, 2.50, 3.00, 4.00, 5.00, and 6.00 s). For each experiment in the frequency list (FQ2LIST), the on-resonance and off-resonance pulses were 403 and 50000 Hz, respectively. Briefly, two free induction decay (FID) data sets were collected in an interleaved manner to minimize temporal fluctuations with the protein irradiation frequency set on-resonance (−0.5 ppm) and off-resonance (40 ppm) (sw = 6000 Hz, 16 steady-state scans, 2048 transients, 4k complex points, d1 = 3 s). Protein saturation was obtained using a train of individual 50 ms long and frequency selective Gaussian radio frequency (rf) pulses separated by an inter-pulse delay of 1 ms. The FID acquired with off-resonance irradiation generated the reference spectrum (I_{off}), whereas the difference FID (off-resonance, on-resonance) yielded the STD spectrum (ISTD = I_{off} - I_{on}). Spectra were processed with an exponential apodization function (1 Hz line broadening) and zero-filling to 8 k complex points before Fourier transformation and baseline correction with a third-order Bernstein polynomial fit. The STD measurements were performed in duplicate, and all data were processed and analysed using TopSpin software (Bruker v 3.5).

5.5 Enzymatic assay and real-time NMR measurements

The FPPS enzyme was produced by gene expression. Substrates of DMAPP ammonium salt and IPP trilithium salt were purchased from Sigma-Aldrich (Italy). A stock buffer solution (25 mM d-Tris, 0.5 mM $MgCl_2$ and 25 mM NaCl, pH 7.4) was made in H_2O and 10% D_2O. Different samples in a standard 5 mm NMR tube were used.

The following factors must be considered for the enzymatic assays: temperature, pH, ionic strength, cofactors, and the proper concentrations of essential components such as substrates and enzymes. The concentration of all substrates directly involved in the enzyme reaction should be saturated so that no component will be rate-limiting. Binding of these components to the enzyme follows a hyperbolic saturation function according to the Michaelis–Menten equation.[65] Therefore, two experiments were performed, one where the concentration of IPP remained fixed (200 μM) and DMAPP varied (25 μM, 50 μM, 75 μM, 100 μM, 125 μM, 150 μM and 200 μM), another where the concentration of DMAPP remained fixed (50 μM) and IPP varied (25 μM, 50 μM, 75 μM, 100 μM, 125 μM, 150 μM and 200 μM). Finally, the concentration of each substrate was supplemented according to their particular K_m value.

The first sample, containing only substrates IPP and DMAPP at a concentration of 400 μM:200 μM (IPP:DMAPP 2:1) and a final volume of 500 μL, was initially used to determine the NMR parameters. The second sample consisted of a kinetic experiment sample containing IPP:DMAPP (2:1 molar ratio) and FPPS enzyme at a concentration of 8 μM. A timer was started to keep track of the delay time before starting the collection of the first NMR spectrum, and the delay time (T0) was added into the following calculations. For the other kinetic experiments, the samples were prepared to contain first IPP:DMAPP in a 2:1 molar ratio and ligands **1**, **2** and **2f** at different concentrations; a timer was started when the FPPS enzyme at a concentration of 8 μM was added.

A one-dimensional NMR experiment was performed on the first sample, containing only substrates, at 37°C to identify the distinct resonances of IPP and DMAPP. Standard pulse calibration was performed to determine the 90° pulse. Each one-dimensional NMR spectrum was collected in a Bruker 600 MHz NMR spectrometer with a spectral width of 19.22 ppm (9615.38 Hz) over 32768 points to provide an acquisition time of 4.14 min per experiment. A relaxation delay of 2 s was used between the scans, and 64 scans were signal-averaged and saved for further processing. This experiment was arrayed to collect FIDs one after another continuously, and a total of 8 such experiments (8 × 4.14 min = 33.12 min) were performed. NMR data were processed and analysed using TopSpin software (Bruker v 3.5).

GraphPad software was used to measure the enzyme kinetics and to determine IC_{50} values. Data were first changed to the logarithmic form and then, using the dose-response-inhibition window, and nonlinear regression curve fit was processed to obtain the kinetic parameters.

5.6 FPPS colorimetric assay

The colorimetric assays were performed in 96-well flat bottom plates. Two hundred nanograms of fresh, pure FPPS was assayed in a final volume of 100 µL buffer (50 mM Tris pH 7.5, 2 mM $MgCl_2$, 1 mM DTT, 5 µg/mL BSA) with or without pre-incubation with inhibitors (**2f** 0.1, 0.5, 1, 2.5, 5 mM and Zol 1, 2.5, 5 µM as positive control) for 30 min at 37°C. The reaction was initiated by the addition of the substrates DMAPP (50 µM) and IPP (50 µM) and proceeded for 1 h at 37°C. Ten microliters of 2.5% ammonium molybdate reagent (in 5 N H_2SO_4) was added and incubated for 10 min to allow the formation of the pyrophosphate(PPi)-molybdate complex. Finally, the complex was reduced by 10 µL of 0.5 M 2-mercaptoethanol and 5 µL of Eikonogen's reagent (0.25 g of sodium sulfite and 14.7 g of meta-bisulfite dissolved in 100 mL of water). The plates were incubated with gentle mixing on a plate shaker for 20 min. The absorbance was measured at 580 nm using a microplate reader. The control experiments were

carried out with an incubation mixture in the absence of substrate or FPPS for background deduction. A standard curve using $Na_2P_2O_7$ as the source of PPi was constructed to set the conditions.

6. Biological assays

6.1 Reagents

Compounds **i6A**, **2** and **2**(**a-m**) were dissolved in DMSO and added to the cell cultures at the reported concentrations. Recombinant human IL-2 protein was purchased from Roche Diagnostics (Indianapolis, IN, USA); Zol and IPP triammonium salt solution were purchased from Sigma–Aldrich.

6.2 mAb and cytofluorimetric analysis

For evaluation of cell expansion, PBMCs were harvested after a 12-14 day culture period and analysed using 2-colour flow cytometry (FACSVerse; Becton Dickinson, Heidelberg, Germany). Fluorescein isothiocyanate (FITC)-conjugated anti-human TCRγδ and phycoerythrin (PE)-conjugated anti-human CD3 monoclonal antibodies (mAbs) were purchased from BD Biosciences (San Jose, CA, USA). BD FACSuite software was used for acquisition and analysis of the flow data expressed as the logarithmic values of fluorescence intensity.

6.3 Cells

For experiments, the human glioma cell lines U87MG (U87) were obtained from CLS Cell Lines Service GmbH (Eppelheim, Germany) or were kindly provided by Dr. Daniela Parolaro (University of Insubria, Italy). U87MG cells were cultured in EMEM (Lonza) supplemented

with 10% heat-inactivated FBS (Euroclone), 1% L-glutamine, 1% antibiotic mixture, 1% sodium pyruvate, and 1% non-essential amino acids (Euroclone).

Healthy peripheral blood mononuclear cells were isolated over Ficoll-Hypaque gradients (MP Biomedicals Aurora, OH, USA). PBMCs were grown in RPMI 1640 (Invitrogen, San Diego, CA, USA) supplemented with 2 mM L-glutamine, 50 ng/mL streptomycin, 50 units/mL penicillin, and 10% heat-inactivated foetal bovine serum (HyClone Laboratories, Logan, UT, USA). All donors gave written informed consent by the Declaration of Helsinki for the use of their residual buffy coats for research purposes with approval from the University Hospital of Salerno Review Board. All cell cultures were maintained at 37°C in a humidified 5% CO_2 atmosphere.

6.4 Determination of GBM cell proliferation

U87MG cells (4×10^3/well) were cultured for 24 h into 96-well plates before the addition of **i6A**, **2** or **2a-m** at the indicated concentrations and cultured for an additional 48 h at 37°C. Cell proliferation was evaluated by measuring BrdU incorporation into DNA (BrdU colorimetric assay kit; Roche Applied Science, South San Francisco, CA). Newly synthesized BrdU-DNA was determined by an ELISA plate reader (Thermo Scientific) at 450 nm. All experiments were performed in triplicate, and the relative cell growth was expressed as a percent compared with the untreated control cells (100%).

6.5 Analysis of viability

Quantitative assessment of PBMC vitality was analysed by PI staining. Briefly, cells were stained with PI at room temperature for 15 min in the dark. The cells were analysed by flow cytometry within 1 h after staining. At least 10 000 events were collected, and the data were analysed by BD FACSuite software (BD Biosciences).

6.6 Expansion of human peripheral blood γδ T Cells

The culture medium for the expansion of human peripheral blood γδ T cells was prepared by adding human IL-2 (IL-2), Zol, IPP or compounds (**i6A**, **2**, **2a-m**) at a final concentration of 150 IU/ml for IL-2 and 5 μM for all other compounds. PBMCs (1×10^6 cells) were cultured in a 24-well plate and were placed in a humidified 37°C, 5% CO_2 incubator for 24-48 h, with the cell culture maintained at a cell density of 0.5-2 × 10^6 cells/mL. Fresh medium containing human IL-2 (150 IU/ml) was added every 2-3 days with the supplementation of serum to the medium to maintain a concentration of at least 1%. Cells were harvested on day 14, and the frequency and phenotype of γδ T cells were determined by flow cytometry.

6.7 Phenotypic analysis by flow cytometry

First, 200 μL of samples containing 2 × 10^5 cells were transferred to fluorescence-activated cell sorting (FACS) tubes and 2 mL of cold PBS was added followed by centrifugation for 5 min at 400 × g. Then, the pellets were re-suspended in 50 μL of FACS buffer (PBS + 1% FCS + 0.1% sodium azide), and the antibodies (anti-TCRγδ and anti-CD3) were added to the samples. Incubation was performed on ice in the dark for 20 min, after which 2 mL of FACS buffer was added to each sample. The samples were centrifuged for 5 min at 400 × g at 4°C, and after decanting the supernatants, the cell pellets were re-suspended in 250 μL of FACS buffer for vortexing. BD FACSuite software was used for the acquisition and analysis of the flow data expressed as logarithmic values of fluorescence intensity.

6.8 Statistical analysis

Statistical analysis was performed in all experiments using GraphPad Prism 6.0 software for Windows (GraphPad software). For each type of assay or phenotypic analysis, data obtained

from multiple experiments were calculated as the mean ± SD and analysed for statistical significance using the two-tailed Student's t-test for independent groups or ANOVA followed by Bonferroni correction for multiple comparisons. P values <0.05 were considered significant. *p<0.05, **p<0.01 and ***p<0.001.

Acknowledgements

This study was supported by the Associazione Italiana Ricerca sul Cancro (AIRC; IG 18999 to M. Bifulco). E.C. was also supported by a triennial fellowship from Fondazione Umberto Veronesi (FUV 2017, cod.1072, FUV 2018, cod.2153 & FUV 2019 cod. 2798).

Author Contributions

A.M.D'U. designed the work. M.S. and M. Buonocore performed the computer-based molecular design. M.R., R.R., and V.C. designed and performed the synthesis of **2a-m**. M.G., I.S., and A.M.D'U. performed and analysed the NMR experiments; A.T., M.G., and I.S. developed the NMR-based enzymatic assay. E.C. and P.G. performed the biochemical tests. A.M.D'U., M. Bifulco, and M.R. supervised the discussion of all results. A.M.D'U. wrote the manuscript. All authors reviewed the manuscript.

Additional Information

Competing financial interests: The authors declare no competing financial interests.

References

[1] J.C. Sacchettini, C.D. Poulter, Biochemistry - Creating isoprenoid diversity, Science 277(5333) (1997) 1788-1789. https://doi.org/10.1126/science.277.5333.1788

[2] A. Szkopinska, D. Plochocka, Farnesyl diphosphate synthase; regulation of product specificity, Acta Biochim. Pol. 52(1) (2005) 45-55. https://doi.org/10/055201045

[3] M.K. Dhar, A. Koul, S. Kaul, Farnesyl pyrophosphate synthase: a key enzyme in isoprenoid biosynthetic pathway and potential molecular target for drug development, New biotechnol. 30(2) (2013) 114-123. https://doi.org/10.1016/j.nbt.2012.07.001

[4] H.Y. Kim, D.K. Kim, S.H. Bae, H. Gwak, J.H. Jeon, J.K. Kim, B.I. Lee, H.J. You, D.H. Shin, Y.H. Kim, S.Y. Kim, S.S. Han, J.K. Shim, J.H. Lee, S.G. Kang, H. Jang, Farnesyl diphosphate synthase is important for the maintenance of glioblastoma stemness, Exp. Mol. Med. 50 (2018). https://doi.org/10.1038/s12276-018-0166-2

[5] F. Ahmad, Q. Sun, D. Patel, J.M. Stommel, Cholesterol Metabolism: A Potential Therapeutic Target in Glioblastoma, Cancers (Basel) 11(2) (2019). https://doi.org/10.3390/cancers11020146
[6] M. Abate, C. Laezza, S. Pisanti, G. Torelli, V. Seneca, G. Catapano, F. Montella, R. Ranieri, M. Notarnicola, P. Gazzerro, M. Bifulco, E. Ciaglia, Deregulated expression and activity of Farnesyl Diphosphate Synthase (FDPS) in Glioblastoma, Sci. Rep. 7(1) (2017) 14123. https://doi.org/10.1038/s41598-017-14495-6
[7] S.A. Holstein, A patent review of bisphosphonates in treating bone disease, Expert Opin. Ther. Pat. (2019) 1-11. https://doi.org/10.1080/13543776.2019.1608180
[8] M. Thurnher, O. Nussbaumer, G. Gruenbacher, Novel Aspects of Mevalonate Pathway Inhibitors as Antitumor Agents, Clin. Cancer Res. 18(13) (2012) 3524-3531. https://doi.org/10.1002/jcc.21334
[9] P.G.J. Fournier, F. Dauhine, M.W. Lundy, M.J. Rogers, F.H. Ebetino, P. Clezardin, Lowering Bone Mineral Affinity of Bisphosphonates as a Therapeutic Strategy to Optimize Skeletal Tumor Growth Inhibition In vivo, Cancer Res 68(21) (2008) 8945-8953. https://doi.org/10.1158/0008-5472.CAN-08-2195
[10] G.J. Morgan, F.E. Davies, W.M. Gregory, K. Cocks, S.E. Bell, A.J. Szubert, N. Navarro-Coy, M.T. Drayson, R.G. Owen, S. Feyler, First-line treatment with zoledronic acid as compared with clodronic acid in multiple myeloma (MRC Myeloma IX): a randomised controlled trial, The Lancet 376(9757) (2010) 1989-1999. https://doi.org/10.1016/S0140-6736(10)62051-X
[11] M. Kondo, K. Sakuta, A. Noguchi, N. Ariyoshi, K. Sato, S. Sato, K. Sato, A. Hosoi, J. Nakajima, Y. Yoshida, K. Shiraishi, K. Nakagawa, K. Kakimi, Zoledronate facilitates large-scale ex vivo expansion of functional gamma delta T cells from cancer patients for use in adoptive immunotherapy, Cytotherapy 10(8) (2008) 842-856. https://doi.org/10.1080/14653240802419328
[12] S. Meraviglia, M. Eberl, D. Vermijlen, M. Todaro, S. Buccheri, G. Cicero, C. La Mendola, G. Guggino, M. D'Asaro, V. Orlando, F. Scarpa, A. Roberts, N. Caccamo, G. Stassi, F. Dieli, A.C. Hayday, In vivo manipulation of Vgamma9Vdelta2 T cells with zoledronate and low-dose interleukin-2 for immunotherapy of advanced breast cancer patients, Clin. Exp. Immunol. 161(2) (2010) 290-7. https://doi.org/10.1111/j.1365-2249.2010.04167.x
[13] E. Lo Presti, G. Pizzolato, A.M. Corsale, N. Caccamo, G. Sireci, F. Dieli, S. Meraviglia, gamma delta T Cells and Tumor Microenvironment: From Immunosurveillance to Tumor Evasion, Front. Immunol. 9 (2018). https://doi.org/10.3389/fimmu.2018.01395
[14] W.K. Tan, J.C. Tay, J. Zeng, M. Zheng, S. Wang, Expansion of Gamma Delta T Cells-A Short Review on Bisphosphonate and K562-Based Methods, (2018). https://doi.org/10.29245/2578-3009/2018/3.1133
[15] S. Sun, C.E. McKenna, Farnesyl pyrophosphate synthase modulators: a patent review (2006–2010), Expert Opin. Ther. Pat. 21(9) (2011) 1433-1451. https://doi.org/10.1517/13543776.2011.593511
[16] J. Park, C.Y. Leung, A.N. Matralis, C.M. Lacbay, M. Tsakos, G. Fernandez De Troconiz, A.M. Berghuis, Y.S. Tsantrizos, Pharmacophore mapping of thienopyrimidine-based monophosphonate (ThP-MP) inhibitors of the human farnesyl pyrophosphate synthase, J. Med. Chem. 60(5) (2017) 2119-2134. https://doi.org/10.1021/acs.jmedchem.6b01888
[17] J. Park, Y.-S. Lin, J.W. De Schutter, Y.S. Tsantrizos, A.M. Berghuis, Ternary complex structures of human farnesyl pyrophosphate synthase bound with a novel inhibitor and secondary ligands provide insights into the molecular details of the enzyme's active site closure, BMC Struct. Biol. 12(1) (2012) 32. https://doi.org/10.1186/1472-6807-12-32
[18] W. Jahnke, J.M. Rondeau, S. Cotesta, A. Marzinzik, X. Pelle, M. Geiser, A. Strauss, M. Gotte, F. Bitsch, R. Hemmig, C. Henry, S. Lehmann, J.F. Glickman, T.P. Roddy, S.J. Stout, J.R. Green, Allosteric non-bisphosphonate FPPS inhibitors identified by fragment-based discovery, Nat. Chem. Biol. 6(9) (2010) 660-666. https://doi.org/10.1038/nchembio.421
[19] A.L. Marzinzik, R. Amstutz, G. Bold, E. Bourgier, S. Cotesta, J.F. Glickman, M. Goette, C. Henry, S. Lehmann, J.C.D. Hartwieg, Discovery of Novel Allosteric Non-Bisphosphonate Inhibitors of Farnesyl Pyrophosphate Synthase by Integrated Lead Finding, Chem. Med. Chem. 10(11) (2015) 1884-1891. https://doi.org/10.1002/cmdc.201500338
[20] M. Scrima, G. Lauro, M. Grimaldi, S. Di Marino, A. Tosco, P. Picardi, P. Gazzerro, R. Riccio, E. Novellino, M. Bifulco, G. Bifulco, A.M. D'Ursi, Structural Evidence of N6-Isopentenyladenosine As a New Ligand of Farnesyl Pyrophosphate Synthase, J. Med. Chem. 57(18) (2014) 7798-7803. https://doi.org/abs/10.1021/jm500869x
[21] M. Bifulco, A.M. Malfitano, M.C. Proto, A. Santoro, M.G. Caruso, C. Laezza, Biological and pharmacological roles of N-6-Isopentenyladenosine: An emerging anticancer drug, Anti-Cancer Agent. Med. Chem. 8(2) (2008) 200-204. https://doi.org/10.2174/187152008783497028
[22] H. Kersten, On the biological significance of modified nucleosides in tRNA, Prog. Nucleic Acid Res. Mol. Biol. 31 (1984) 59-114. https://doi.org/10.1016/s0079-6603(08)60375-x
[23] H.M. Laten, S. Zahareasdoktor, Presence and Source of Free Isopentenyladenosine in Yeasts, Proc. Natl. Acad. Sci. U. S. A. 82(4) (1985) 1113-1115. https://doi.org/10.1073/pnas.82.4.1113

[24] K. Doležal, I. Popa, E. Hauserová, L. Spíchal, K. Chakrabarty, O. Novák, V. Kryštof, J. Voller, J. Holub, M. Strnad, Preparation, biological activity and endogenous occurrence of N6-benzyladenosines, Bioorg. Med. Chem. 15(11) (2007) 3737-3747. https://10.1016/j.bmc.2007.03.038
[25] C. Laezza, A. D'Alessandro, L. Di Croce, P. Picardi, E. Ciaglia, S. Pisanti, A.M. Malfitano, M. Comegna, R. Faraonio, P. Gazzerro, M. Bifulco, p53 regulates the mevalonate pathway in human glioblastoma multiforme, Cell Death Dis. 6 (2015). https://doi.org/10.1038/cddis.2015.279
[26] C. Laezza, M.G. Caruso, T. Gentile, M. Notarnicola, A.M. Malfitano, T. Di Matola, C. Messa, P. Gazzerro, M. Bifulco, N6-isopentenyladenosine inhibits cell proliferation and induces apoptosis in a human colon cancer cell line DLD1, Int. J.Cancer 135(10) (2014) E11-E11. https://doi.org/10.1038/cddis.2015.279
[27] I.S. Woo, S.Y. Eun, H.J. Kim, E.S. Kang, H.J. Kim, J.H. Lee, K.C. Chang, J.H. Kim, S.C. Hong, H.G. Seo, Farnesyl diphosphate synthase attenuates paclitaxel-induced apoptotic cell death in human glioblastoma U87MG cells, Neurosci. Lett. 474(2) (2010) 115-120. https://doi.org/10.1016/j.neulet.2010.03.021
[28] S. Castiglioni, S. Casati, R. Ottria, P. Ciuffreda, J.A.M. Maier, N6-Isopentenyladenosine and its Analogue N6-Benzyladenosine Induce Cell Cycle Arrest and Apoptosis in Bladder Carcinoma T24 Cells, Anti-Cancer Agent. Med. Chem. 13(4) (2013) 672-678. https://doi.org/10.2174/1871520611313040016
[29] E. Ciaglia, C. Laezza, M. Abate, S. Pisanti, R. Ranieri, A. D'alessandro, P. Picardi, P. Gazzerro, M. Bifulco, Recognition by natural killer cells of N6-isopentenyladenosine-treated human glioma cell lines, Int. J.Cancer 142(1) (2018) 176-190. https://doi.org/10.1002/ijc.31036
[30] E. Ciaglia, M. Grimaldi, M. Abate, M. Scrima, M. Rodriquez, C. Laezza, R. Ranieri, S. Pisanti, P. Ciuffreda, C. Manera, P. Gazzerro, A.M. D'Ursi, M. Bifulco, The isoprenoid derivative N(6) -benzyladenosine CM223 exerts antitumor effects in glioma patient-derived primary cells through the mevalonate pathway, Br. J. Pharmacol. 174(14) (2017) 2287-2301. https://doi.org/10.1111/bph.13824
[31] A. Santoro, E. Ciaglia, V. Nicolin, A. Pescatore, L. Prota, M. Capunzo, M.V. Ursini, S.L. Nori, M. Bifulco, The isoprenoid end product N6-isopentenyladenosine reduces inflammatory response through the inhibition of the NF kappa B and STAT3 pathways in cystic fibrosis cells, Inflamm.Res. 67(4) (2018) 315-326. https://doi.org/10.1007/s00011-017-1123-6
[32] E. Ciaglia, S. Pisanti, P. Picardi, C. Laezza, A.M. Malfitano, A. D'Alessandro, P. Gazzerro, M. Vitale, E. Carbone, M. Bifulco, N6-isopentenyladenosine, an endogenous isoprenoid end product, directly affects cytotoxic and regulatory functions of human NK cells through FDPS modulation, J. Leukoc. Biol. 94(6) (2013) 1207-1219. https://doi.org/10.1189/jlb.0413190
[33] E. Ciaglia, S. Pisanti, P. Picardi, C. Laezza, S. Sosa, A. Tubaro, M. Vitale, P. Gazzerro, A.M. Malfitano, M. Bifulco, N6-isopentenyladenosine affects cytotoxic activity and cytokines production by IL-2 activated NK cells and exerts topical anti-inflammatory activity in mice, Pharmacol.Res. 89 (2014) 1-10. https://doi.org/10.1016/j.phrs.2014.07.003
[34] J.M. Rondeau, F. Bitsch, E. Bourgier, M. Geiser, R. Hemmig, M. Kroemer, S. Lehmann, P. Ramage, S. Rieffel, A. Strauss, Structural basis for the exceptional in vivo efficacy of bisphosphonate drugs, Chem. Med. Chem. 1(2) (2006) 267-273. https://doi.org/10.1002/cmdc.200500059
[35] K.L. Kavanagh, K. Guo, J.E. Dunford, X. Wu, S. Knapp, F.H. Ebetino, M.J. Rogers, R.G. Russell, U. Oppermann, The molecular mechanism of nitrogen-containing bisphosphonates as antiosteoporosis drugs, Proc. Natl. Acad. Sci.U. S. A. 103(20) (2006) 7829-34. https://doi.org/10.1073/pnas.0601643103
[36] O. Trott, A.J. Olson, AutoDock Vina: improving the speed and accuracy of docking with a new scoring function, efficient optimization, and multithreading, J. Comput. Chem. 31(2) (2010) 455-61. https://doi.org/10.1002/jcc.21334
[37] S. Bhattarai, M. Freundlieb, J. Pippel, A. Meyer, A. Abdelrahman, A. Fiene, S.Y. Lee, H. Zimmermann, G.G. Yegutkin, N. Strater, A. El-Tayeb, C.E. Muller, alpha,beta-Methylene-ADP (AOPCP) Derivatives and Analogues: Development of Potent and Selective ecto-5'-Nucleotidase (CD73) Inhibitors, J. Med. Chem. 58(15) (2015) 6248-63. https://10.1021/acs.jmedchem.5b00802
[38] Y.A. Kim, A. Sharon, C.K. Chu, R.H. Rais, O.N. Al Safarjalani, F.N. Naguib, M.H. el Kouni, Synthesis, biological evaluation and molecular modeling studies of N6-benzyladenosine analogues as potential anti-toxoplasma agents, Biochem. Pharmacol. 73(10) (2007) 1558-72. https://10.1016/j.bcp.2007.01.026
[39] J. Ravn, K. Qvortrup, C. Rosenbohm, T. Koch, Design, synthesis, and biological evaluation of LNA nucleosides as adenosine A3 receptor ligands, Bioorg. Med. Chem. 15(16) (2007) 5440-7. https://10.1016/j.bmc.2007.05.056
[40] T. Fujii, T. Saito, The Dimroth rearrangement of 9-substituted 1-methyladenines: accelerating effect of a beta-D-ribofuranosyl group at the 9-position, Nucleic Acids Symp. Ser. (16) (1985) 69-72.
[41] R. Ottria, S. Casati, E. Baldoli, J.A. Maier, P. Ciuffreda, N(6)-Alkyladenosines: Synthesis and evaluation of in vitro anticancer activity, Bioorg. Med. Chem. 18(23) (2010) 8396-402. https://10.1016/j.bmc.2010.09.030
[42] J. Charton, S. Girault-Mizzi, M.-A. Debreu-Fontaine, F. Foufelle, I. Hainault, J.-G. Bizot-Espiard, D.-H. Caignard, C. Sergheraert, Synthesis and biological evaluation of benzimidazole derivatives as potent AMP-

activated protein kinase activators, Bioorg. Med. Chem. 14(13) (2006) 4490-4518. https://10.1016/j.bmc.2006.02.028
[43] D. Tarkowská, K. Doležal, P. Tarkowski, C. Åstot, J. Holub, K. Fuksová, T. Schmülling, G. Sandberg, M. Strnad, Identification of new aromatic cytokinins in Arabidopsis thaliana and Populus× canadensis leaves by LC-(+) ESI-MS and capillary liquid chromatography/frit–fast atom bombardment mass spectrometry, Physiol. Plant. 117(4) (2003) 579-590. https://doi.org/10.1023/A:1015027906046
[44] P. Štarha, I. Popa, Z. Trávníček, J. Vančo, N6-Benzyladenosine derivatives as novel N-donor ligands of platinum (II) dichlorido complexes, Molecules 18(6) (2013) 6990-7003. https://10.3390/molecules18066990
[45] R. Randino, E. Cini, A.M. D'Ursi, E. Novellino, M. Rodriquez, Facile Baeyer–Villiger oxidation of cyclic ketones: conventional versus microwave-assisted approach, Tetrahedron Lett. 56(42) (2015) 5723-5726. https://doi.org/10.1016/j.tetlet.2015.08.082
[46] J.B. Chen, E.M. Liu, T.R. Chern, C.W. Yang, C.I. Lin, N.K. Huang, Y.L. Lin, Y. Chern, J.H. Lin, J.M. Fang, Design and Synthesis of Novel Dual-Action Compounds Targeting the Adenosine A2A Receptor and Adenosine Transporter for Neuroprotection, Chem. Med. Chem. 6(8) (2011) 1390-1400. https://doi.org/10.1002/cmdc.201100126
[47] P.T. Anastas, J.C. Warner, Green chemistry: theory and practice, Oxford university press Oxford2000.
[48] A. de la Hoz, A. Diaz-Ortiz, A. Moreno, Microwaves in organic synthesis. Thermal and non-thermal microwave effects, Chem. Soc. Rev. 34(2) (2005) 164-178. https://doi.org/10.1039/b411438h
[49] M.T. Nevalainen, V.C. Njar, Z. Liao, A.B. Reitz, M.E. McDonnell, Treatment of prostate cancer and hematologic neoplasms, Google Patents, 2015.
[50] R. Randino, E. Cini, A.M. D'Ursi, E. Petricci, M. Rodriquez, Synthesis and biological evaluation of small Molecules derivatives of the natural Histone deacetylase inhibitor FR235222, PharmacologyOnLine 3 (2014) 203-208.
[51] M. Mayer, B. Meyer, Characterization of ligand binding by saturation transfer difference NMR spectroscopy, Angew. Chem. Int. Ed. 38(12) (1999) 1784-1788. https://doi.org/10.1002/(SICI)1521-3773(19990614)38:12<1784::AID-ANIE1784>3.0.CO;2-Q
[52] M. Mayer, B. Meyer, Group epitope mapping by saturation transfer difference NMR to identify segments of a ligand in direct contact with a protein receptor, J. Am. Chem. Soc. 123(25) (2001) 6108-6117. https://doi.org/10.1021/ja0100120
[53] O. Cala, F. Guillière, I. Krimm, NMR-based analysis of protein–ligand interactions, Anal. Bioanal. Chem. 406(4) (2014) 943-956. https://doi.org/10.1007/s00216-013-6931-0
[54] J. Angulo, P.M. Nieto, STD-NMR: application to transient interactions between biomolecules-a quantitative approach, Eur. Biophys. J. 40(12) (2011) 1357-1369. https://doi.org/10.1007/s00249-011-0749-5
[55] Y.S. Wang, D. Liu, D.F. Wyss, Competition STD NMR for the detection of high-affinity ligands and NMR-based screening, Magn. Reson. Chem. 42(6) (2004) 485-489. https://doi.org/10.1002/mrc.1381
[56] M. Arro, D. Manzano, A. Ferrer, Farnesyl diphosphate synthase assay, Methods Mol. Biol. 1153 (2014) 41-53. https://doi.org/10.1007/978-1-4939-0606-2_4
[57] G. Prism, Graphpad software, San Diego, CA, USA (1994).
[58] J. Gao, X. Chu, Y. Qiu, L. Wu, Y. Qiao, J. Wu, D. Li, Discovery of potent inhibitor for farnesyl pyrophosphate synthase in the mevalonate pathway, Chem. Commun. 46(29) (2010) 5340-5342. https://doi.org/10.1039/c0cc00992j
[59] S. Lindert, W. Zhu, Y.L. Liu, R. Pang, E. Oldfield, J.A. McCammon, Farnesyl diphosphate synthase inhibitors from in silico screening, Chem. Biol. Drug Des. 81(6) (2013) 742-748. https://doi.org/10.1111/cbdd.12121
[60] D. Gritzalis, J. Park, W. Chiu, H. Cho, Y.-S. Lin, J.W. De Schutter, C.M. Lacbay, M. Zielinski, A.M. Berghuis, Y.S. Tsantrizos, Probing the molecular and structural elements of ligands binding to the active site versus an allosteric pocket of the human farnesyl pyrophosphate synthase, Bioorg. Med. Chem. Lett. 25(5) (2015) 1117-1123. https://doi.org/10.1016/j.bmcl.2014.12.089
[61] C.Y. Leung, J. Park, J.W. De Schutter, M. Sebag, A.M. Berghuis, Y.S. Tsantrizos, Thienopyrimidine bisphosphonate (ThPBP) inhibitors of the human farnesyl pyrophosphate synthase: optimization and characterization of the mode of inhibition, J. Med. Chem. 56(20) (2013) 7939-7950. https://doi.org/10.1021/jm400946f
[62] M. Ceccarelli, F.P. Barthel, T.M. Malta, T.S. Sabedot, S.R. Salama, B.A. Murray, O. Morozova, Y. Newton, A. Radenbaugh, S.M. Pagnotta, S. Anjum, J.G. Wang, G. Manyam, P. Zoppoli, S. Ling, A.A. Rao, M. Grifford, A.D. Cherniack, H.L. Zhang, L. Poisson, C.G. Carlotti, D.P.D. Tirapelli, A. Rao, T. Mikkelsen, C.C. Lau, W.K.A. Yung, R. Rabadan, J. Huse, D.J. Brat, N.L. Lehman, J.S. Barnholtz-Sloan, S. Zheng, K. Hess, G. Rao, M. Meyerson, R. Beroukhim, L. Cooper, R. Akbani, M. Wrensch, D. Haussler, K.D. Aldape, P.W. Laird, D.H. Gutmann, H. Noushmehr, A. Iavarone, R.G.W. Verhaak, T.R. Network, Molecular Profiling Reveals Biologically Discrete Subsets and Pathways of Progression in Diffuse Glioma, Cell 164(3) (2016) 550-563. https://doi.org/10.1016/j.cell.2015.12.028

[63] A.J. Roelofs, M. Jauhiainen, H. Monkkonen, M.J. Rogers, J. Monkkonen, K. Thompson, Peripheral blood monocytes are responsible for gammadelta T cell activation induced by zoledronic acid through accumulation of IPP/DMAPP, Br. J. Haematol. 144(2) (2009) 245-50. https://doi.org/10.1111/j.1365-2141.2008.07435.x
[64] P.P. Wizard, M. Maestro, I.F. Phase, Jaguar, and Glide, Schrödinger, LLC: Portland, OR (2009).
[65] L. Michaelis, M.L. Menten, K.A. Johnson, R.S. Goody, The original Michaelis constant: translation of the 1913 Michaelis-Menten paper, Biochemistry 50(39) (2011) 8264-9. https://doi.org/10.1021/bi201284u

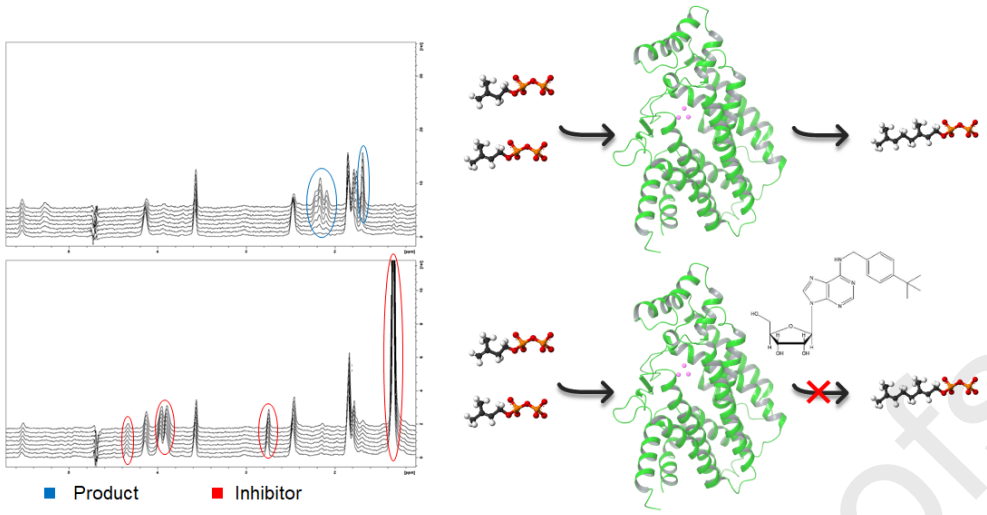

Highlights:

- Farnesyl pyrophosphate synthase is a key enzyme with a significant role in the maintenance of neoplastic malignant phenotype.
- Design and synthesis of selective inhibitors to overcome the pharmacokinetic limits of Nitrogen-Containing Bisphophonates.
- Development of an enzymatic assay based on nuclear magnetic spectroscopy for the evaluation of the K_D.

Declaration of Competing Interest

Competing financial interests: The authors declare no competing financial interests.